

## Center pivot irrigation capacity effects on maize yield and profitability in the Texas High Plains

Alfonso Domínguez<sup>a</sup>, Robert C. Schwartz<sup>b,\*</sup>, José J. Pardo<sup>a</sup>, Bridget Guerrero<sup>c</sup>, Jourdan M. Bell<sup>d</sup>, Paul D. Colaizzi<sup>b,1</sup>, R. Louis Baumhardt<sup>b,1</sup>

<sup>a</sup> Escuela Técnica Superior de Ingenieros Agrónomos y de Montes (ETSIAM), Centro Regional de Estudios del Agua (CREA), Universidad de Castilla-La Mancha (UCLM), Ctra. de Las Peñas, km 3.2, 02071 Albacete, Spain

<sup>b</sup> USDA-ARS, PO Drawer 10, Bushland, TX 79012, USA

<sup>c</sup> Dept. of Agricultural Sciences, West Texas A&M University, Canyon, TX 79016, USA

<sup>d</sup> Texas A&M AgriLife Research & Extension, 6500 Amarillo Blvd W Amarillo, TX 79106, USA

### ARTICLE INFO

Handling Editor - Dr R Thompson

#### Keywords:

Limited irrigation  
MOPECO  
Sprinkler irrigation  
Typical meteorological year  
Water productivity  
*Zea mays* L

### ABSTRACT

In the Texas High Plains (THP), groundwater resources for irrigation are declining because of aquifer depletion and reduced well yield. Inability to meet peak water demands of maize under constrained irrigation capacities decreases yield and profitability. The MOPECO crop model, calibrated for the THP, was adapted to simulate maize water use and yield under center pivot irrigation to evaluate water allocation strategies under limited irrigation. Simulations were carried out over a range of irrigation capacities (3 – 12 mm d<sup>-1</sup> for a 50.9 ha area), initial soil water contents, and application depths with irrigation allocated to a fraction (0.5 – 1.0) of the pivot area. Fractional water allocations were achieved by withholding irrigation from circular sectors or from outer spans with unirrigated fractions in fallow or planted to dryland cotton. These strategies were evaluated for growing seasons characterized by typical meteorological years with average (TMY1), average to above average (TMY2), and below average (TMY3) precipitation. Preseason irrigation had little to no influence on grain yield at irrigation capacities  $\geq 5$  mm d<sup>-1</sup>. At irrigation capacities  $\leq 6$  mm d<sup>-1</sup> under TMY1, marginally greater yields 50.9 ha<sup>-1</sup> were simulated when a fraction was irrigated. For irrigation capacities  $\leq 8$  mm d<sup>-1</sup> under TMY1, reducing the irrigated area was the most prudent option to optimize net returns. As irrigation capacities increased from 4 to 8 mm d<sup>-1</sup>, the irrigated fraction that maximized net returns increased from 0.5 to 0.9. Concentrating water generated greater net returns because of greater irrigation water productivities and lower seed and fertilizer costs. Compared with fallow, planting cotton in the unirrigated portion increased net returns except in years with a seasonal drought (TMY3). Because greater irrigation volume did not always increase net returns, there is an opportunity to both increase profitability and conserve water by irrigating a fraction of the area.

### 1. Introduction

The High Plains aquifer is a major source of water for irrigation, industrial uses, and drinking water throughout the U.S. Great Plains and extends from the Texas High Plains (THP) to Nebraska and South Dakota. Approximately 24 billion m<sup>3</sup> was pumped from the aquifer in 2005 of which 97% was used for irrigation on roughly 6.3 million ha of farmland (McGuire, 2009). In the southern portion of the High Plains aquifer, pumping has greatly exceeded recharge rates resulting in declines in saturated thickness exceeding 46 m in extensive areas of southern Kansas and the THP since predevelopment (McGuire, 2017).

Decreases in saturated thickness increase the pumping cost but more importantly reduce the well yield. Declining well flow capacities reduces both crop yield and profitability because peak water use usually coincides with crop reproductive stages when water stress results in the greatest yield reductions (Scanlon et al., 2012; Foster et al., 2015; Schwartz et al., 2020a). Because of the severity aquifer depletion, water management strategies such as changing crop type, irrigation scheduling, and conversion to dryland are being evaluated for economic feasibility and effectiveness in prolonging the life of irrigated agriculture in the THP (Crouch et al., 2020).

Maize (*Zea mays* L.) accounts for approximately 50% of pumping for

\* Corresponding author.

<sup>1</sup> USDA is an Equal Opportunity Provider and Employer.

irrigation (Colaizzi et al., 2009; Schlegel et al., 2012; Xue et al., 2017) and has seasonal water requirements ranging from 670 to 970 mm in the THP (Howell et al., 1995b, 1996; Schneider and Howell, 1998; Schwartz et al., 2020a). Because of maize sensitivity to water deficits, marginal well capacities that reduce irrigation allocations during critical growth stages can result in considerable reductions in grain yield (Howell et al., 1996; Schwartz et al., 2020a).

In 2000, for approximately 72% of the irrigated area in the THP, water was delivered to crops using center pivot irrigation systems (Colaizzi et al., 2009). From 1958–2000, the number of wells in the THP doubled however during this same time period, the seasonal volume of water pumped per well and the area irrigated per well was cut in half (Colaizzi et al., 2009). With an average irrigated area per well of 18 ha in 2000, typically three wells are required to irrigate a quarter section (~51 ha). When adding more wells is not an option or cost prohibitive, the operator runs the system at reduced flow rates, which oftentimes requires changing nozzles to lower flow rates or turning off a certain number of nozzles to maintain system pressure. Flow rates of  $1.68 \text{ m}^3 \text{ h}^{-1} \text{ ha}^{-1}$  (3 gal  $\text{min}^{-1} \text{ ac}^{-1}$ ) are common in the region. Because a flow rate of  $1.68 \text{ m}^3 \text{ h}^{-1} \text{ ha}^{-1}$  can only deliver  $4.0 \text{ mm d}^{-1}$ , operators slow down the pivot speed to increase the application volume resulting in a period of over 6 days to apply 25 mm irrigation. Given daily reference evapotranspiration ( $ET_0$ ) values of 8 mm and often exceeding 10 mm a day combined with unreliable precipitation, it is obvious that these flow rates are insufficient to meet water requirements of maize throughout much of the growing season. Scheduling irrigation to maintain soil water above a certain stress threshold is usually not attainable under these conditions except during periods of above average precipitation (Mahan and Lascano, 2016). Preseason irrigation (Schlegel et al., 2012) and irrigating above crop requirements during the early vegetative stage are common strategies that producers use to build plant available water in the deep soils characteristic of the region. Stored soil water is used later in the growing season during peak water use periods to partially offset insufficient irrigation capacity.

An evaluation of maize yield and profit as influenced by limited irrigation capacities should consider the wide inter-annual variabilities in growing season precipitation and  $ET_0$ . Considering these constraints, the principal management option producers have available to them is how to distribute water spatially within a field, managing a portion under deficit or full irrigation with the remaining area planted to a dryland crop or left fallow. Secondary management considerations include (i) varying the pivot speed to adjust the depth of application and consequently the time between irrigations and (ii) choosing how to reduce the irrigated acreage by either supplying water only to a sector of the pivot circle (Baumhardt et al., 2007) or by shutting off nozzles on the outer spans of the pivot and thereby reducing radius of the irrigated area. Crops suitable for dryland production may also be planted on acreage that is not irrigated.

The objective of this study is to utilize a calibrated crop water use and yield model to optimize planted acreage and management practices that would maximize long-term total maize yield and profitability for a center pivot irrigated 50.9 ha field over a range of irrigation capacities. A secondary objective is to determine optimal management interventions to mitigate losses in years with extended seasonal drought.

## 2. Methodology

### 2.1. Climate data and analysis

Climatic data extending from 1993 to 2018 at the USDA-ARS Conservation and Production Research Laboratory (Bushland, TX, 1170 m asl;  $35^{\circ}11' \text{ N}$ ,  $102^{\circ}6' \text{ W}$ ) were used in these evaluations. The weather station is centered within an irrigated cool season grass surface described by Howell et al. (1995a). Solar irradiance, wind speed, air temperature, dew point temperature, relative humidity, and barometric pressure were monitored at this weather station throughout the year and

precipitation were measured with tipping bucket rain gages over the grass surface. In these analyses, the years 2012, 2013, and 2015 were omitted because of uncertainties in the quality of data during the growing season. Using this weather data,  $ET_0$  was calculated using the ASCE standardized reference evapotranspiration equation for a short reference crop at a 24-h time step (ASCE, 2005).

In the THP, maize is typically planted from late April to mid-May and the initiation of the dough stage (R4) for a crop planted in mid-May will typically occur on 28 August based on mean growing degree days for the period of record. Consequently, climatic data for a growing season extending from 1 May to 28 August is the most crucial for determining irrigation requirements and maize yield potential. Precipitation and weather conditions extending from R4 to physiological maturity (~17 Sept.) has a comparatively minor influence on the yield potential (Schwartz et al., 2020a). From 1939–2018, mean precipitation at the Bushland research station for the period 1 May to 28 August was 264 mm (S.D. = 95.6 mm) and the data exhibits a strong normal distribution (Shapiro-Wilk  $p = 0.661$  (Fig. 1a). From 1993–2018, mean precipitation and  $ET_0$  was 231 and 874 mm, respectively, during this critical time period.

Because the U.S. Southern Great Plains is prone to extreme droughts, it is important to differentiate years that exhibit lower than normal precipitation from years with normal to above average precipitation. Combined with reliable drought forecasts, the assessment of irrigation requirements in these years could provide actionable information for producers and also crop insurance providers to adjust the planted acreage, reduce crop failures, reduce unproductive water consumption, and increase profit. The Oceanic Niño Index temperature anomaly associated with La Niña is not a good predictor of summer droughts in the southern U.S. Great Plains (Pu et al., 2016) and this observation is supported by the climatic data at the Bushland station with only 2 of 5 La Niña years exhibiting cumulative precipitation for the period 1 May to 28 Aug that could be considered to be a seasonal drought (Fig. 1b). More importantly, for the climatic data at Bushland (1993 – 2018), the Oceanic Niño Index temperature anomaly for May–July is uncorrelated ( $r = 0.002$ ; slope =  $-0.0005$ ) to the precipitation/ $ET_0$  ratio (not shown), an indicator of seasonal irrigation requirements.

We consider drought within the growing season as those years with precipitation falling within the 0.8–1.0 exceedance probabilities as evaluated using the long-term precipitation record in Bushland (Fig. 1b). This threshold also corresponds to a standardized precipitation index ( $(x - \bar{x})/\sigma$ ) of  $< -0.84$  utilized by Agnew (2000) to identify years with at least a moderate to severe level of drought. More importantly, this threshold segregates years that exhibit elevated temperatures and evaporative demands that, in addition to below normal precipitation, are associated with droughts in the region. In normal to wet years with exceedance probabilities  $< 0.80$ ,  $ET_0$  varied little with respect to seasonal precipitation averaging 820 mm and increasing 0.3 mm for every 1 mm decline in precipitation ( $p = 0.08$ ; Fig. 1c). Above this threshold,  $ET_0$  increased 2.6 mm for every 1 mm decline in precipitation ( $p < 0.001$ ; Fig. 1c). The relationship between increasing  $ET_0$  with decreasing precipitation is characteristic of droughts in the Southern U. S. Great Plains and is a product of the coupling of land surface soil moisture and precipitation. Soil moisture deficits in the spring increase sensible heating and surface temperatures thereby increasing evaporative demands and oftentimes leading to convective inhibition and a reduction in precipitation (Fernando et al., 2019).

Use of a typical meteorological year (TMY) is useful for planning and assessing irrigation requirements because of the great degree of uncertainty in year to year forecasted precipitation during the growing season (Domínguez et al., 2013). A TMY consists of one year of climatic data chosen from a long time series typically spanning more than 10 years (Hall et al., 1978).

Using the 1993–2018 climatic data in Bushland, TX, TMY's were constructed using (i) all years to evaluate the mean response (TMY1), (ii) years with precipitation exceedance probabilities less than 0.8 and

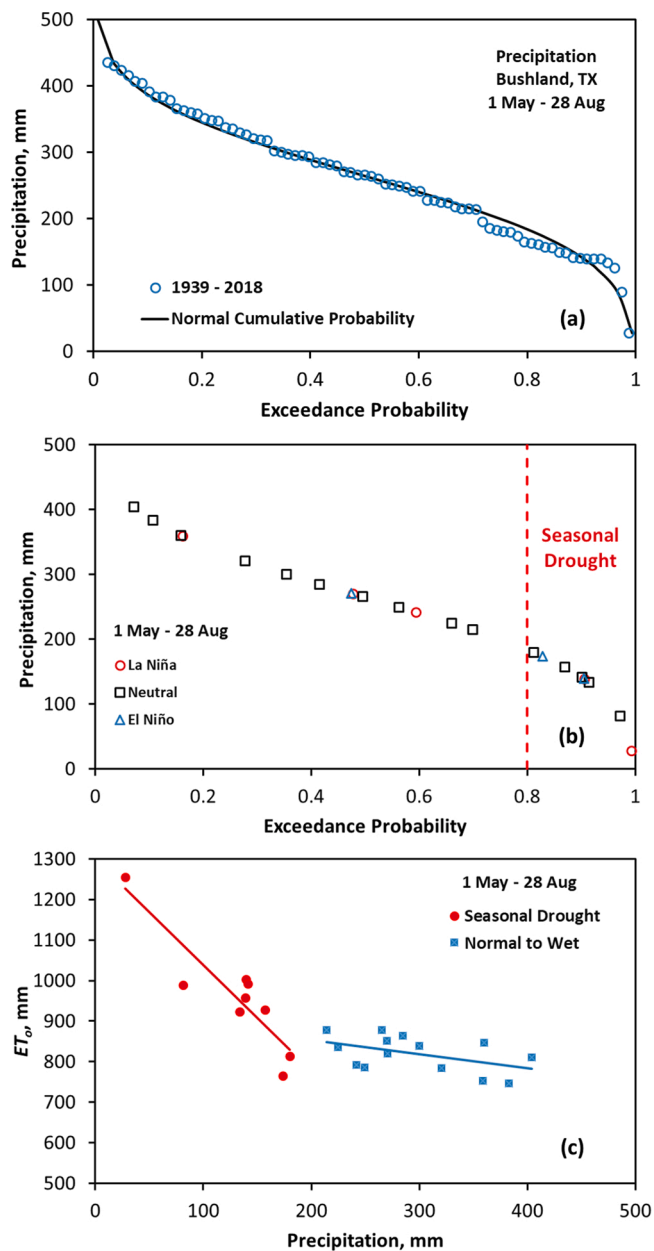


**Fig. 1.** (a) Precipitation exceedance probability from 1939 to 2018 in Bushland, TX and the normal cumulative probability function for the mean (264 mm) and standard deviation (95.6 mm); (b) Precipitation exceedance probability from 1993 to 2018 in Bushland, TX in relation to the Oceanic Niño Index (ONI) anomalies averaged over May through July (El Niño  $\leq -0.5$  °C;  $-0.5 < \text{Neutral} < 0.5$ ; La Niña  $\geq +0.5$  °C). Also shown is the threshold established to identify seasonal droughts for the period of 1 May to 28 Aug; (c) Relationship between seasonal precipitation and reference ET ( $ET_0$ ) at the Bushland, TX station from 1993 to 2018.

regarded as growing seasons with normal to above average precipitation (TMY2), and years with precipitation exceedance probabilities greater than 0.8 and regarded as growing seasons with a pronounced drought (TMY3). Each of these three scenarios were developed using climatic data extending from 1 May to 31 October with each of the “typical” months chosen by Finkelstein-Schafer statistical comparisons of candidate monthly periods with long-term cumulative distribution frequencies of maximum and minimum temperatures, precipitation, and  $ET_0$  (Domínguez et al., 2013).

## 2.2. Crop water use and yield model

The crop water use and yield model MOPECO (model for the economic optimization of irrigation water) (Ortega et al., 2004) with the modifications introduced by Schwartz et al. (2020a) was used to simulate maize water use and yield in response to center pivot irrigation scenarios in the THP. MOPECO uses the FAO-56 crop coefficient – reference ET approach (FAO, 1998) in conjunction with an empirical crop water production function to predict grain yield. The yield function is based on the work of Stewart et al. (1977) and Doorenbos and Kassam (1979) that considers water deficits at different crop growth stages in a multiplicative relationship (Rao et al., 1988; Domínguez et al., 2012a, 2012b).

The crop model was calibrated and validated using 18 site-years that consisted of detailed water use monitored throughout each growing season determined with a soil water balance approach and a neutron gage to evaluate changes in stored soil water (Schwartz et al., 2020a). Maize yields of the calibration data set ranged from 0 to 19.3 Mg ha<sup>-1</sup> with crop water use that ranged from 310 mm (dryland) to 770 mm. Crop phenological growth stages associated with crop coefficients (Schwartz et al., 2020a; Fig. 1c) were estimated using growing degree days (GDD) for each TMY. Growing degree days were evaluated using daily maximum and minimum temperatures with a 10 °C base temperature and an upper temperature threshold of 30 °C using Method 2 of McMaster and Wilhelm (1997). In this study, we used the fixed and fitted parameters for the nonlinear crop water stress function (Schwartz et al., 2020a; Optimization 3) to simulate maize water use and yield. Soil water retention and other parameters used in these simulations are for a Pullman clay loam (Fine, mixed, superactive, thermic Torrertic Paleustoll) (Schwartz et al., 2020a) and, along with two other soils series with nearly identical properties, represent the principal soil groups used for maize production in the THP.

Crop water use and yield simulations of MOPECO were implemented in an Excel spreadsheet with a fixed planting date of 16 May. Redistribution of water from infiltrated precipitation,  $P$ , and irrigation,  $I$ , within the rooting zone occurs instantaneously, and drainage out of the rooting zone occurs when the soil water content exceeds field capacity. The maximum rooting depth of the maize, attained at inflorescence, was set equivalent to 1.4 m. The initial water content was set equivalent to 0.278 m<sup>3</sup> m<sup>-3</sup> for the entire profile, which was based on the mean of initial water contents in the data sets evaluated by Schwartz et al. (2020a). Runoff depth,  $R$ , from daily precipitation depth,  $P$ , was estimated using the original curve number approach (Rallison, 1980),

$$R = \begin{cases} (P - I_a)^2 / (P - I_a + S_I) & P > I_a \\ 0 & P \leq I_a \end{cases} \quad (1)$$

where  $S_I$  is the potential retention due to soil water storage or infiltration, whichever is the least, and the depth of initial abstraction,  $I_a$ , is set to 15 mm. Because near surface soil water content could not be approximated using the Excel spreadsheet redistribution algorithm of MOPECO as in Schwartz et al. (2020a),  $S_I$  was set to a constant value of 23.1 mm. This assumes that the upper 0.2 m of the profile had an initial water content equivalent to 75% plant available water, which was similar to observed values for irrigated maize (Schwartz et al., 2020a). Net irrigation,  $I_N$ , was estimated as in Schwartz et al. (2020a) by multiplying the gross application depth,  $I_G$ , by an application efficiency,  $AE_I$ , of 0.90 (Howell, 2003). If the gross application depth was less than a threshold  $d_0 = 25$  mm, then net irrigation was estimated as  $I_G - d_0 \cdot (1 - AE_I)$  to account for diminishing application efficiencies associated with evaporative losses with shallow application depths (Schwartz et al., 2020a).

The crop water use and yield simulations use the weather data of the TMY’s that reflect growing seasons with average, normal to above average, and below average (drought) growing season precipitation. As such, these simulations reflect the expected mean response over the

long-term. A limited number of crop model simulations were also carried out for all climatic data (1993–2018) to validate the TMY approach in the southern U.S. Great Plains environment and also to provide an assessment of the variability of the predicted yield response and net returns. In each year of these simulations, crop developmental stages were based on growing degree days calculated from daily minimum and maximum temperatures in each of the growing seasons. In addition, yield response was scaled based on the accumulated solar radiation after pollination in each year, with a scalar of unity for the average solar radiation accumulation for all years. As with the simulations using the TMY's, we completed these simulations using a planting date of 16 May.

2.3. Adaptation of the crop water use and yield model for selected scenarios

Crop water use, yield response, and net returns were evaluated using the crop water use and yield model and four center pivot irrigation scenarios or strategies for a quarter mile (402 m) long pivot or approximately 50.9 ha (Table 1). These evaluations were carried out using the three TMY's reflecting growing seasons with average, normal to above average, and below average (drought) growing season precipitation. For the typical management (Strategy 1 "S1") we considered 10 irrigation capacities (3, 4, 5, 12 mm d<sup>-1</sup>) generated by a single well or a group of wells for the irrigation of the entire area of a standard center pivot system. These irrigation capacities were evaluated in conjunction with three initial profile water contents (0.278 ± 0.0278 m<sup>3</sup> m<sup>-3</sup>) representing the mean and ± 1 standard deviation, respectively, of 18 site-years of studies presented by Schwartz et al. (2020a). An incremental increase in initial profile water content from 0.278 to 0.306 m<sup>3</sup> m<sup>-3</sup> was considered representative of sufficient pre-irrigation to increase stored soil water at planting by 38.9 mm and achieved through three irrigations of 25 mm several weeks before planting. A net increase of 25 mm stored soil water with 50 mm of irrigation applied is characteristic of the fine-textured soils in the region (Tolk et al., 2015). The standard management strategy (S1) was compared with the other strategies to determine if yield and profitability could be improved (Table 1).

A second strategy considered (S2) varies the irrigation application depth from 15 to 35 mm at the 10 irrigation capacities with application depth constant throughout the entire growing season (Table 1). This strategy permits an evaluation of how different application depths influence crop yield. Smaller application depths permit the crop to receive

irrigation over smaller time intervals but this comes with the disadvantage of reduced application efficiency.

Besides irrigating the entire circle, producers have the option of leaving a fraction of the circle unirrigated when irrigation capacities become limiting (Baumhardt et al., 2007, 2009). The unirrigated area can be left fallow or planted to a dryland crop. Strategy 3 (S3) reduces the area irrigated by the pivot by supplying water to all nozzles but withholding irrigation to one or more sectors of the circle (Table 1). This strategy permits an increase in the irrigation frequency; however, irrigation is delayed by the time it takes for the pivot to travel through the unirrigated sectors at its maximum speed (100%), assumed here as one full rotation per day (0.083 rad h<sup>-1</sup>) or 1.76 m min<sup>-1</sup> at the outermost nozzle. In Scenario 3, irrigating in different directions is avoided and the irrigation system must travel across the non-irrigated area to commence irrigation on the first sector.

A fourth strategy (S4) reduces the irrigated area by turning off nozzles on the outer spans of the pivot (Table 1). In this case, the nozzle flow rates, travel speed, and irrigation frequency are increased in order to maintain a selected application depth. All strategies are evaluated with regard to seasonal irrigation requirements, grain yield, and irrigation water productivity with respect to the maize crop. Evaluation of net returns requires inclusion of how the unirrigated fraction is cropped and managed under strategies 3 and 4.

2.4. Irrigation scheduling simulations for a center pivot

Decisions to irrigate must reflect the available irrigation capacity, the speed of the center pivot drive, the irrigated area, and if there is sufficient water holding capacity near the surface to store the water applied. To simplify the simulation process, the irrigated area is divided into 10 sectors for all strategies (Table 1). A daily water balance and likewise a crop water stress level are maintained throughout the entire growing season in each of the 10 sectors. Irrigation is first applied to the first sector and then to the remaining sectors and always in the same order. However, if precipitation and/or ET<sub>o</sub> are favorable and the irrigation capacity is more than sufficient to meet crop water requirements, irrigation is applied only when stored crop available water is ≤ 70% of available water at field capacity associated with the maximum rooting depth of the crop. Although at times, the system may be applying more than is required by the crop, producers use this strategy to store water that could be used later in the growing season when ET<sub>o</sub> is greater.

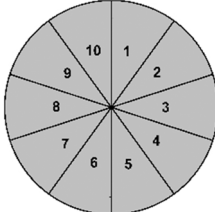
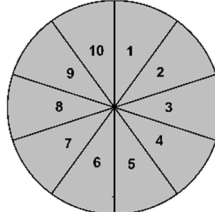
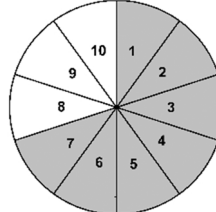
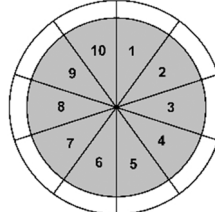
Table 1

Evaluated irrigation strategies and conditions for a center pivot with 10 circular sectors. The shape of the irrigated area is shown for an irrigated fraction of 0.7 for both strategy S3 (reducing number of sectors irrigated) and strategy S4 (reducing the irrigated radius).

Strategy	S1	S2	S3	S4
Pivot area, ha	50.9	50.9	50.9	50.9
Irrigation capacities, mm d <sup>-1a</sup>	3–12	3–12	3–12	3–12
Flow capacities, m <sup>3</sup> h <sup>-1a</sup>	63.6–254.3	63.6–254.3	63.6–254.3	63.6–254.3
Decline in capacity (%)	0 and 15	0 and 15	0 and 15	0 and 15
Initial Water Content, m <sup>3</sup> m <sup>-3</sup>	0.250, 0.278, 0.306	0.278	0.278	0.278
Application depth, mm	25	15, 20, 25, 30, 35	25	25
Irrigated Fraction (Sector) <sup>b</sup>	1.0	1.0	0.5–1.0	1.0
Irrigated Fraction (Radius) <sup>b</sup>	1.0	1.0	1.0	0.5–1.0
Crop Production	Irrigated Maize	Irrigated Maize	Irrigated Maize, Dryland Cotton, Fallow	Irrigated Maize, Dryland Cotton, Fallow

Shape of irrigated area (shaded)

<sup>a</sup> Irrigation capacities examined were 3, 4, 5, 6, 7, 8, 9, 10, 11, and 12 mm d<sup>-1</sup> equivalent to 63.6–254.3 m<sup>3</sup> h<sup>-1</sup> and 2.2–8.9 gal min<sup>-1</sup> ac<sup>-1</sup>.

<sup>b</sup> Irrigated fractions examined were 0.5, 0.6, 0.7, 0.8, 0.9, and 1.0.

Irrigation is also not applied within one week prior to black layer. Because a mean water balance is maintained in each of the sectors, crop yield is also simulated for each of these sectors.

During the growing season, groundwater levels in observation wells will typically decline by two to four meters (North Plains Groundwater Conservation District, 2020; Stout, 2018), reaching a minimum in August and rebounding to near initial levels later in the growing season. These declines in groundwater levels are principally driven by irrigation decisions of producers with nearby actively pumped wells. Such seasonal perturbations can be considered as a temporary decline in the saturated thickness of the aquifer in the immediate vicinity and is largely responsible for reduced pumping capacities during the growing season as experienced by producers in the region. Within the model, we assume a linear reduction in irrigation capacity by 15% from emergence to the beginning of August and a constant reduction of 15% thereafter, extending to maturity, to account for these seasonal changes in groundwater levels. This magnitude of decline during the growing season is representative of many wells in the North THP that draw water from the aquifer (Personal communication, Dale Hallmark, North Plains Groundwater Conservation District). To our knowledge, these types of limits on well yield have never been incorporated into a crop model during the growing season.

Irrigation at the prescribed depth is triggered when plant available water is less than or equal to 70% of plant available water and when the center pivot is positioned at the beginning of the first sector. This can be written as

$$Irrigate = \begin{cases} True & \text{if } \begin{cases} S_{PA} \leq 0.7 \cdot S_{fc} \\ \text{and} \\ \Theta = 0 \end{cases} \\ False & \text{otherwise} \end{cases} \quad (2)$$

where  $S_{PA}$  is the plant available soil water within the profile (mm) associated with the maximum rooting depth, and  $S_{fc}$  is the plant available soil water at field capacity (mm). The angular position of the pivot is described by  $\Theta$  (rad) with the area of sector 1 circumscribed between 0 and  $2\pi/10$ . Based on the fraction of the pivot that is irrigated under strategy 3 (Table 1), a contiguous circular sector of the pivot area beginning with sector 1 is designated as a subset of irrigated sectors with the remaining area designated as a subset of unirrigated sectors. The gross irrigation depth,  $I_G$ , is fixed throughout the growing season; however, irrigation capacity restricts the volume of irrigation applied in a single day. The volume of irrigation ( $m^3$ ),  $V_i$ , applied to sector  $i$  ( $s_i$ ) is calculated as

$$V_i = \begin{cases} 0 \\ \text{Min} \left[ 10 \cdot A \cdot I_G \cdot \left( \frac{s_i}{n_s} - \frac{\Theta_{i-1}}{2\pi} \right), \frac{A \cdot q}{f_r} \cdot (1 - T_{i-1}) \right] \end{cases} \quad \text{if } \begin{cases} \Theta < 2\pi \cdot (s_i - 1) / n_s \text{ and } \Theta \geq 2\pi \cdot s_i / n_s \\ \text{or} \\ T \geq 1 \\ \text{or} \\ s_i \subseteq \text{unirrigated sectors} \end{cases} \quad (3)$$

The volume applied  $V_i$  is spread over the surface area at a depth of  $I_G$  that may not comprise the entire area of the sector if there is insufficient capacity within a day to complete irrigation of a given sector. Here,  $n_s$  is the number of sectors (10),  $q$  is the irrigation capacity ( $mm \text{ d}^{-1}$ ) for the total area of the pivot ( $A = 50.9 \text{ ha}$ ), and  $f_r$  is the fraction of the area that is irrigated when the reduction of irrigated area is achieved by turning off nozzles in the outer spans (Strategy 4; Table 1). In this case, the area associated with decreased radius increases the effective irrigation capacity to  $q/f_r$ . In addition,  $T_{i-1}$  and  $\Theta_{i-1}$  are the time (d) and angular position (rad), respectively, prior to initiation of irrigation in sector  $s_i$ . Assuming that irrigation has been triggered and there is time remaining within the day, the pivot applies irrigation to the subsequent sector and so on until  $T = 1$  upon which  $T$  is reset to zero for the next day of simulations. Cumulative time,  $T_i$ , after the pivot has traveled within a sector  $s_i$  is

$$T_i = \begin{cases} T_{i-1} + \frac{V_i}{A \cdot n_s \cdot q} & \text{if } s_i \subseteq \text{irrigated sectors} \\ T_{i-1} + \text{Min} \left[ f_{100} \cdot \left( \frac{s_i}{n_s} - \frac{\Theta_{i-1}}{2\pi} \right), 1 - T_{i-1} \right] & \text{if } s_i \subseteq \text{unirrigated sectors} \end{cases} \quad (4)$$

where  $T_{i-1}$  is the time at the completion of the previous sector,  $q$  is the irrigation capacity ( $mm \text{ d}^{-1}$ ),  $f_{100}$  is the maximum rotational frequency ( $\text{d}^{-1}$ ) associated with movement of the pivot over unirrigated surfaces, and  $\Theta_{i-1}$  is the radial position of the pivot after completing movement through the previous sector or, if there was insufficient time to complete irrigation in the previous day, the position within the current sector. The radial position of the pivot at time  $T_i$  is

$$\Theta_i = \begin{cases} \Theta_{i-1} + \frac{V_i \cdot 2\pi}{A \cdot I_G \cdot n_s} & \text{if } s_i \subseteq \text{irrigated sectors} \\ \Theta_{i-1} + \frac{2\pi \cdot (T_i - T_{i-1})}{f_{100}} & \text{if } s_i \subseteq \text{unirrigated sectors} \end{cases} \quad (5)$$

We note that the irrigation capacity  $q$  is constant for a given day but can decline on subsequent days because of the simulated reduced pumping capacities later in the growing season (Table 1).

### 2.5. Economic analysis

The application of the crop water use and yield model within a center

**Table 2**  
Crop production revenue and variable costs.

Crop production	Irrigated Maize	Dryland Cotton	Fallow
<b>Revenue from sale</b>			
Harvested grain, \$ Mg <sup>a</sup>	165.00		
Lint, \$ kg <sup>a</sup>		1.50	
Cotton seed <sup>a</sup> , \$ kg <sup>a</sup>		0.22	
<b>Variable Costs</b>			
Seed <sup>a</sup> , \$ ha <sup>a</sup>	296.25	167.19	
Herbicide, \$ ha <sup>a</sup>	111.20	97.75	59.58
Harvest aid (defoliant), \$ ha <sup>a</sup>		24.71	
Insecticide and fungicide, \$ ha <sup>a</sup>	55.67	25.23	
Fertilizer, pre-plant N, \$ kg <sup>a</sup>	1.10	1.10	
Fertilizer, UAN (32–0–0), \$ kg <sup>a</sup>	0.97		
Fertilizer, pre-plant P <sub>2</sub> O <sub>5</sub> , \$ kg <sup>a</sup>	1.06	1.06	
Pre-plant fertilizer application, \$ ha <sup>a</sup>	13.02	13.02	
Custom harvest and hauling grain, \$ Mg <sup>a</sup>	8.27		
Stripping, module, and ginning cotton, \$ bale <sup>a</sup> (226.8 kg)		46.35	
Irrigation pumping costs (energy), \$ 100·m <sup>-3</sup>	3.50	3.50	
Irrigation labor, \$ ha <sup>a</sup>	44.73		
Machinery labor, \$ ha <sup>a</sup>	32.54	49.95	8.54
Diesel fuel and gasoline, \$ ha <sup>a</sup>	33.30	32.51	5.13
Repairs and maintenance, \$ ha <sup>a</sup>	254.05	55.67	11.42
Crop consulting, \$ ha <sup>a</sup>	20.34		
Crop insurance, \$ ha <sup>a</sup>	99.21	61.78	
Boll weevil assessment, \$ ha <sup>a</sup>		1.83	
Interest on credit line, \$ ha <sup>a</sup>	31.23	20.04	2.89

<sup>a</sup> Cotton seed yield was set equivalent to 1.2 × lint yield.

<sup>b</sup> Planting rate was set equal to 79,000 and 125,000 seeds ha<sup>-1</sup> for maize and cotton, respectively.

pivot field facilitates the evaluation of potential producer net returns as influenced by irrigation capacity under the conditions of TMY's that reflect growing seasons with average, normal to above average, and below average (drought) growing season precipitation. Calculated net returns, *NR*, (\$ ha<sup>-1</sup>) were based on modeled water inputs and cost estimates:

$$NR = \frac{1}{A} (Y_m \cdot HP_m \cdot A_I + Y_{cl} \cdot HP_{cl} \cdot A_{UI} + Y_{cs} \cdot HP_{cs} \cdot A_{UI} - A_I \cdot C_{vm} - A_{UI} \cdot C_{vc} - A_{UI} \cdot C_{vf}) - I_{GA} \cdot C_w \quad (6)$$

where *NR* reflects the weighted average net returns across the center pivot field (*A* = 50.9 ha), including both irrigated and dryland portions. Here *Y<sub>m</sub>* is maize yield (kg ha<sup>-1</sup>) in the irrigated area of the field, *A<sub>I</sub>*, *HP<sub>m</sub>* is the harvest sale price of maize (\$ kg<sup>-1</sup>) assuming a 15.5% moisture content, *Y<sub>cl</sub>* is dryland cotton lint yield (kg ha<sup>-1</sup>) on the unirrigated area of the field, *A<sub>UI</sub>*, which receives irrigation only for establishment, and *HP<sub>cl</sub>* is the harvest price of cotton lint (\$ kg<sup>-1</sup>). Also, *Y<sub>cs</sub>* is cotton seed yield (kg ha<sup>-1</sup>), assumed here as 1.2 · *Y<sub>cl</sub>*, and *HP<sub>cl</sub>* is the harvest price of cotton seed (\$ kg<sup>-1</sup>). Here *C<sub>vm</sub>*, *C<sub>vc</sub>*, and *C<sub>vf</sub>* represent variable costs (\$ ha<sup>-1</sup>) associated with maize production, dryland cotton, and fallow, respectively, including crop insurance. Lastly *I<sub>GA</sub>* is the cumulative irrigation volume applied by the irrigation system for pre-irrigation and during the growing season (m<sup>3</sup> ha<sup>-1</sup>) averaged over the entire pivot area and *C<sub>w</sub>* is the per unit pumping cost for irrigation water (\$ m<sup>-3</sup>). Based on a study at the location (Schwartz et al., 2020b), cotton was assumed to yield 2.5 kg ha<sup>-1</sup> lint per mm total precipitation received from 1 May to 30 Sep., which corresponds to 575, 788, and 305 kg ha<sup>-1</sup> for TMY1, TMY2, and TMY3, respectively.

The net returns for this analysis represent net returns above variable costs and include only variable costs of production (Table 2) such as fertilizer, seed, herbicide and insecticide applications, crop consulting, and custom harvest. Fixed costs (e.g. depreciation and interest on equipment investment) are not considered in this analysis. Irrigation costs are calculated based on the fuel or energy costs to pump the

applied water volume of gross irrigation. Irrigation repair and labor costs are also considered. Crop prices, production costs, and other production enterprise assumptions used in this study reflect three year averages (2019–2021) (Benavidez et al., 2019, 2020; Jones et al., 2018). Nitrogen fertilizer applications for maize were based on grain yields predicted using the 50% upper confidence interval of yield (*Y<sub>50</sub>*, Mg ha<sup>-1</sup>) for the linear regression of yield with irrigation and seasonal precipitation using the data of Schwartz et al. (2020a).

$$Y_{50} = \text{MIN}(0.02745 \cdot (I_G + P_{ave}) - 4.398, 19) \quad (7)$$

where *I<sub>G</sub>* is cumulative gross irrigation of the area planted to maize (mm ha<sup>-1</sup>) and *P<sub>ave</sub>* is mean seasonal (1 May to 28 Aug) precipitation (264 mm). A 50% upper confidence interval for yield is used to estimate N applications to avoid risk associated with low application rates in years with abundant precipitation. The yield expectations are restricted to a maximum of 19 Mg ha<sup>-1</sup>. Based on these assumptions, applied N (*N<sub>a</sub>*, kg ha<sup>-1</sup>) was calculated as

$$N_a = Y_{50} \cdot 17.86 - 50 \quad (8)$$

assuming a nitrogen rate of 17.86 kg N Mg<sup>-1</sup> grain (1.1 lb N bu<sup>-1</sup>) and available soil N of 50 kg ha<sup>-1</sup>. Assuming an N:P ratio in maize grain of 6.2:1, phosphorus fertilizer applications rates were calculated as

$$P_a = \text{Max}(N_a / 6.2, 11) \quad (9)$$

with a minimum of 11 kg P ha<sup>-1</sup> (25 kg P<sub>2</sub>O<sub>5</sub> ha<sup>-1</sup>) for starter fertilizer. Fertilizer rates for dryland cotton were assumed to be 25 kg P<sub>2</sub>O<sub>5</sub> ha<sup>-1</sup> and 33 kg N ha<sup>-1</sup> (1.2 kg seed kg<sup>-1</sup> lint · 788 kg lint ha<sup>-1</sup> · 35 g N kg<sup>-1</sup> seed). For strategies where a portion of the acreage is planted to dryland cotton, we include the costs of a single irrigation of 25 mm at the beginning of the growing season to guarantee establishment (Table 2).

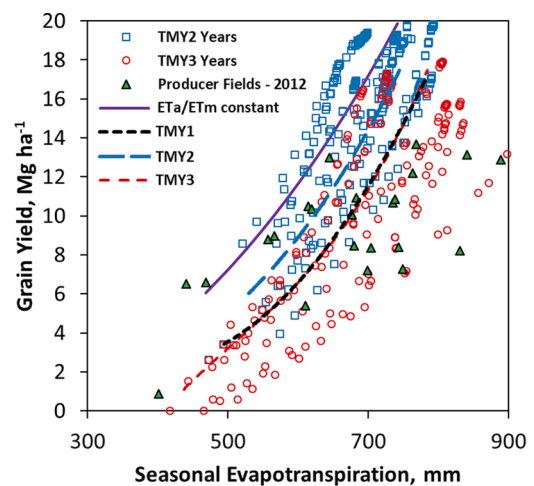


**Fig. 2.** Predicted maize grain yield as a function of seasonal crop evapotranspiration (*ET<sub>a</sub>*) from 1993 to 2018 by TMY grouping simulated for irrigation capacities ranging from 3 to 12 mm d<sup>-1</sup>, an initial profile water content of 0.278 m<sup>3</sup> m<sup>-3</sup> and both 0% and 15% reductions in seasonal irrigation capacities. Also shown is the quadratic response for each TMY (dashed lines). Yields and approximate seasonal ET are also shown for producer fields in the North THP (North Plains Groundwater Conservation District, 2012) in 2012, a drought year with an average of 137 mm precipitation during the growing season. Also shown is the yield response to irrigation applied to achieve a constant fractional *ET<sub>a</sub>/ET<sub>m</sub>* among all growth stages (solid line) for a growing season represented by TMY1.

### 3. Results

#### 3.1. Evaluation of the Typical Meteorological Years

The effective growing season precipitation (precipitation less runoff from planting to physiological maturity) for the typical meteorological years were 158, 268, and 100 mm for TMY1, TMY2, and TMY3, respectively. Crop water requirements during this same period ( $\sum ET_m$ ) did not differ substantially among the TMY's (781, 727, and 795 mm for TMY1, TMY2, and TMY3, respectively) and fell within the observed range for the THP for maize (670–970 mm).

Predicted maize grain yield as a function of seasonal crop evapotranspiration ( $ET_a$ ) from 1993 to 2018 exhibited a wide swath of points

for each TMY (Fig. 2) with years segregated as either TMY2 or TMY3 (Fig. 1c) and noting that all years corresponds to TMY1. These data were generated using simulations in each year (1993 – 2018) with an initial profile water content of  $0.278 \text{ m}^3 \text{ m}^{-3}$ , reductions of seasonal irrigation capacities by 0% and 15%, and by varying irrigation capacities from 3 to  $12 \text{ mm d}^{-1}$ . Grain yields and approximate seasonal ET are also shown for producer fields in the North THP (North Plains Groundwater Conservation District, 2012) in 2012, a drought year with an average of 137 mm precipitation during the growing season. These independent data show a similar pattern and fall within the range delineated by TMY3 simulations representing years with a seasonal drought.

Predicted grain yield response to  $ET_a$  was obtained by fitting a regression line for simulated results obtain for each TMY under S1

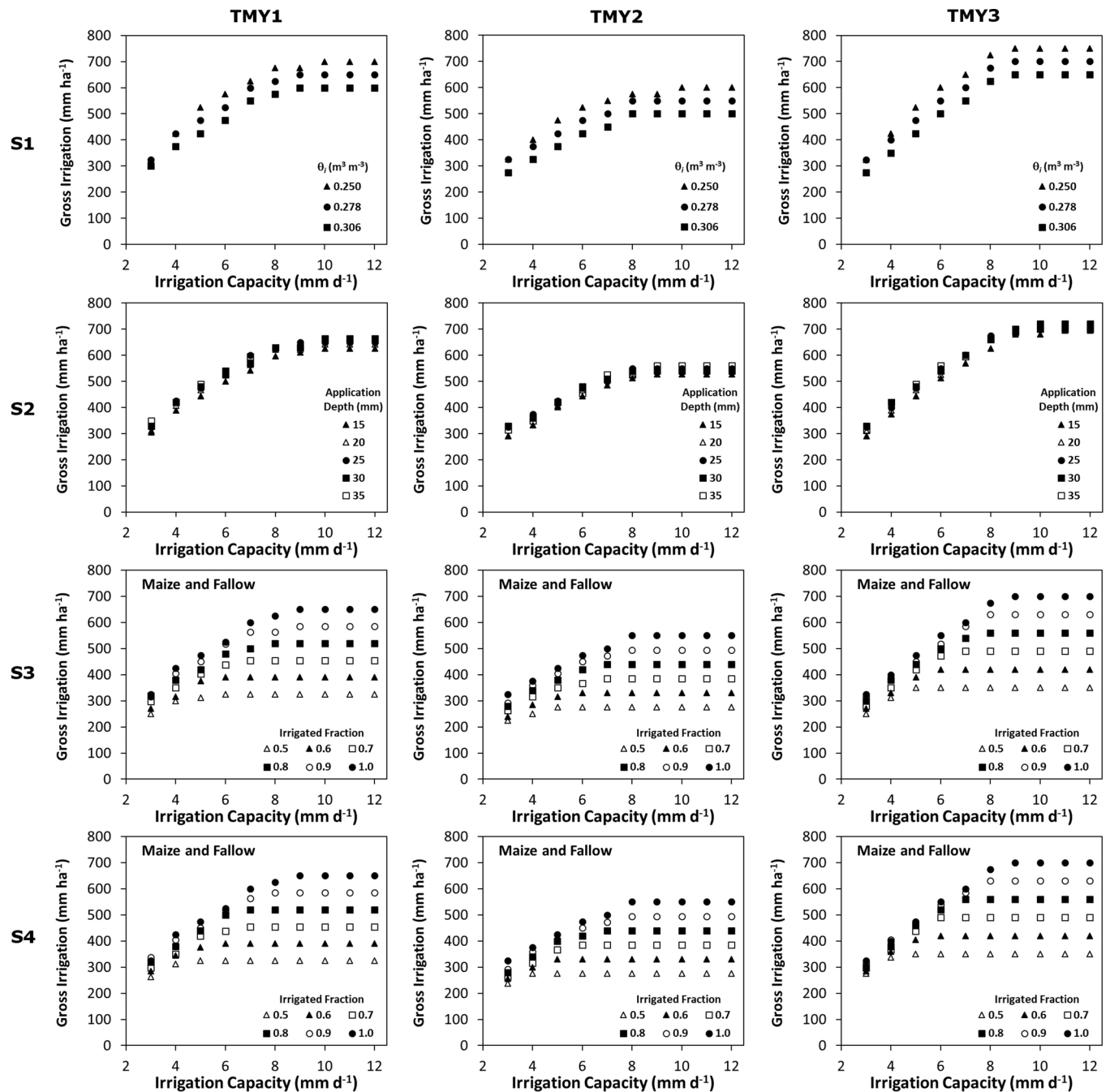


Fig. 3. Calculated gross irrigation applied to the center pivot area by irrigation strategy (rows S1, S2, S3, and S4) and typical meteorological year (columns TMY1, TMY2, and TMY3). Gross irrigation is the applied volume averaged over the entire area of the pivot and not just the irrigated fraction in S3 and S4. Decline in irrigation capacity during the growing season was set to 15% for all simulations.

(Table 1). Yield response was nonlinear with a significant quadratic response ( $P < 0.001$ ) for all TMY's (Fig. 2). The predicted trend of yield with seasonal crop ET for TMY2 and TMY3 falls near the mid-range of the respective model results for all years (1993 – 2018) segregated by TMY grouping (Fig. 2). The TMY associated with above average precipitation (TMY2) had a similar yield response slope but greater yields under the same  $ET_a$  compared with TMY1 and TMY3. This outcome is largely explained by the fact that TMY2 had greater precipitation during July (82 mm) compared with TMY1 (48 mm) and TMY3 (25 mm) and  $ET_a$  as a fraction of maximum ET without stress ( $ET_m$ ) could be maintained at higher levels under TMY2 even with limiting irrigation capacities. During the month of July, the crop is at the early reproductive stage and grain yield is more sensitive to water deficits. Management that applies irrigation to achieve a constant fractional  $ET_a/ET_m$  among all growth stages for a TMY1 growing season resulted in greater predicted yields compared with management restricted by irrigation capacity (Fig. 2). Consequently, past research that maintains a constant ET fraction ( $ET_a/ET_m$ ), typically characteristic of irrigation studies in the U. S. Great Plains, may not be particularly relevant to understanding the yield response of maize when irrigation capacities are limited.

### 3.2. Calculated seasonal irrigation applied to the pivot

Seasonal crop water requirements ( $\sum ET_m$ ) were calculated as 780, 727, and 795 mm ha<sup>-1</sup> under the typical meteorological years TMY1, TMY2, and TMY3, respectively. In contrast, calculated net irrigation applications plus effective precipitation under S1 with initial profile water contents of 0.274 m<sup>3</sup> m<sup>-3</sup> ranged from 451 to 743, 561–763, and 393–730 mm ha<sup>-1</sup> for TMY1, TMY2, and TMY3. Consequently, there was considerable water deficit stress at the low irrigation capacities under all TMY's. Although irrigation at the high capacities could hypothetically meet seasonal irrigation requirements, during the early reproductive phases when  $ET_o$  was high (>9 mm d<sup>-1</sup>) the calculated stress response function predicted water stress above plant available water fractions  $S_{PA}/S_{fc} > 0.7$  (Schwartz et al., 2020a). However, irrigation is not triggered until  $S_{PA}/S_{fc} \leq 0.7$  (Eq. 2) thereby resulting in crop water requirements not fully met during this period even at high capacities. Delaying irrigation is necessary to avoid difficulties with deep wheel tracks and runoff associated with applying irrigation too frequently in the fine-textured soils of the region. Seasonal gross irrigation application rates under S1 varied from 275 to 750 mm depending on the irrigation capacity, TMY, and the initial profile water content (Fig. 3). At irrigation capacities  $\leq 8$  mm d<sup>-1</sup>, a 15% decline in capacity during the growing season reduced the number of irrigations by one to three applications

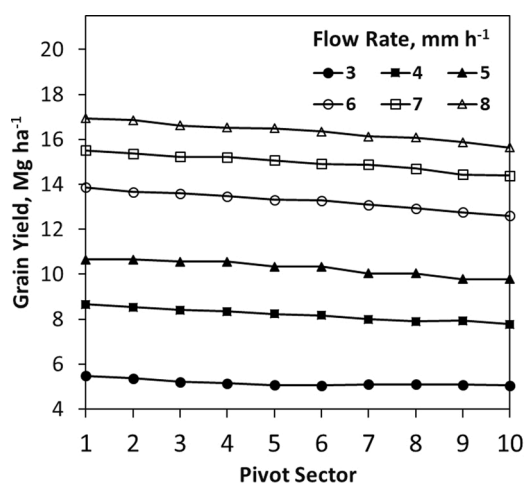


Fig. 4. Grain yield of maize across pivot sectors for TMY1 and strategy S1, an initial profile water content of 0.278 m<sup>3</sup> m<sup>-3</sup> and a 0% decline in irrigation capacity throughout the growing season.

(25–75 mm) compared to strategies with no decline. Increasing application depths from 15 to 35 mm under TMY1 increased seasonal gross irrigation by an average of 37 mm (Fig. 3; S2). Differences in seasonal gross applications among higher application depths (25–35 mm) were, on average, negligible (6 mm) with application depths of 25 and 30 mm sometimes receiving greater total irrigation (Fig. 3) simply as a result of fortuitous timing that permitted an additional one or two revolutions.

Under strategies 3 and 4, only a fraction of the pivot area is irrigated to permit greater application depths on a smaller area and with the remaining pivot area under dryland cotton or fallow. Gross irrigation applications under these two strategies are presented in Fig. 3 as average volumes of the entire area of the pivot and not just the irrigated area. Consequently, maximum seasonal gross irrigation at high capacities obtained when only a fraction is irrigated is less than when the entire area is irrigated. Nonetheless, maximum or near maximum application depths on a fraction of the pivot area could be achieved at lower capacities. Under S4 and for irrigated fractions,  $f_r$ , less than 0.8, an additional one to two irrigation applications (25–50 mm) could be scheduled compared with S3. This result is due to the delay in irrigation associated with moving the pivot through the unirrigated sectors under S3.

### 3.3. Yield response to irrigation strategies

Grain yield for irrigated maize was simulated for each of the 10 sectors of the pivot under all strategies. Yield consistently declined with increasing angular distance from pivot sector 1 (Table 1), which was irrigated first, and resulted in a mean yield difference of 0.93 Mg ha<sup>-1</sup> between sector 1 and 10 (Fig. 4). This yield decline is simply a result of irrigation delays with increasing sector number and associated lower stored soil water throughout most of the growing season that increased water stress and reduced crop ET. This demonstrates that yields at the field scale will be considerably overestimated without considering the temporal-spatial dynamics associated with irrigating. In the remaining discussion, all yield results reported reflect the average of all irrigated sectors.

A 15% simulated decline in the irrigation capacity reduced simulated grain yields by an average of 1.6 Mg ha<sup>-1</sup> for irrigation capacities  $\leq 8$  mm d<sup>-1</sup> (Fig. 5). At greater flow rates, declines in irrigation capacity did not reduce the number of applications and consequently had an insignificant effect on yield. We caution that these yield declines resulting from reduced pumping could be underestimated because they do not consider reduced application uniformity resulting from a degradation of system performance at lower pressures (Martin et al., 2019). Because declines in irrigation capacity throughout the growing season is

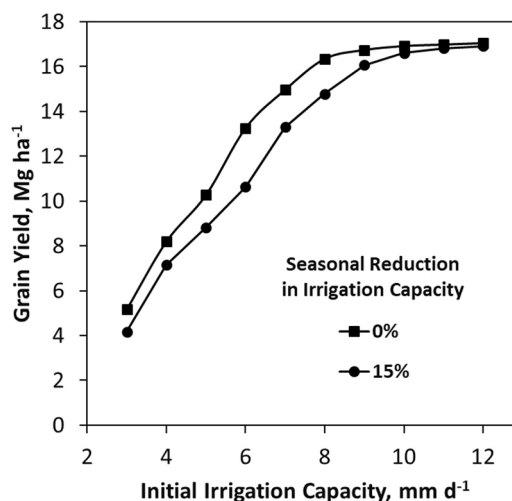


Fig. 5. Effect of a seasonal reduction in irrigation capacity on maize grain yield for TMY1, strategy S1, and an initial profile water content of 0.278 m<sup>3</sup> m<sup>-3</sup>.



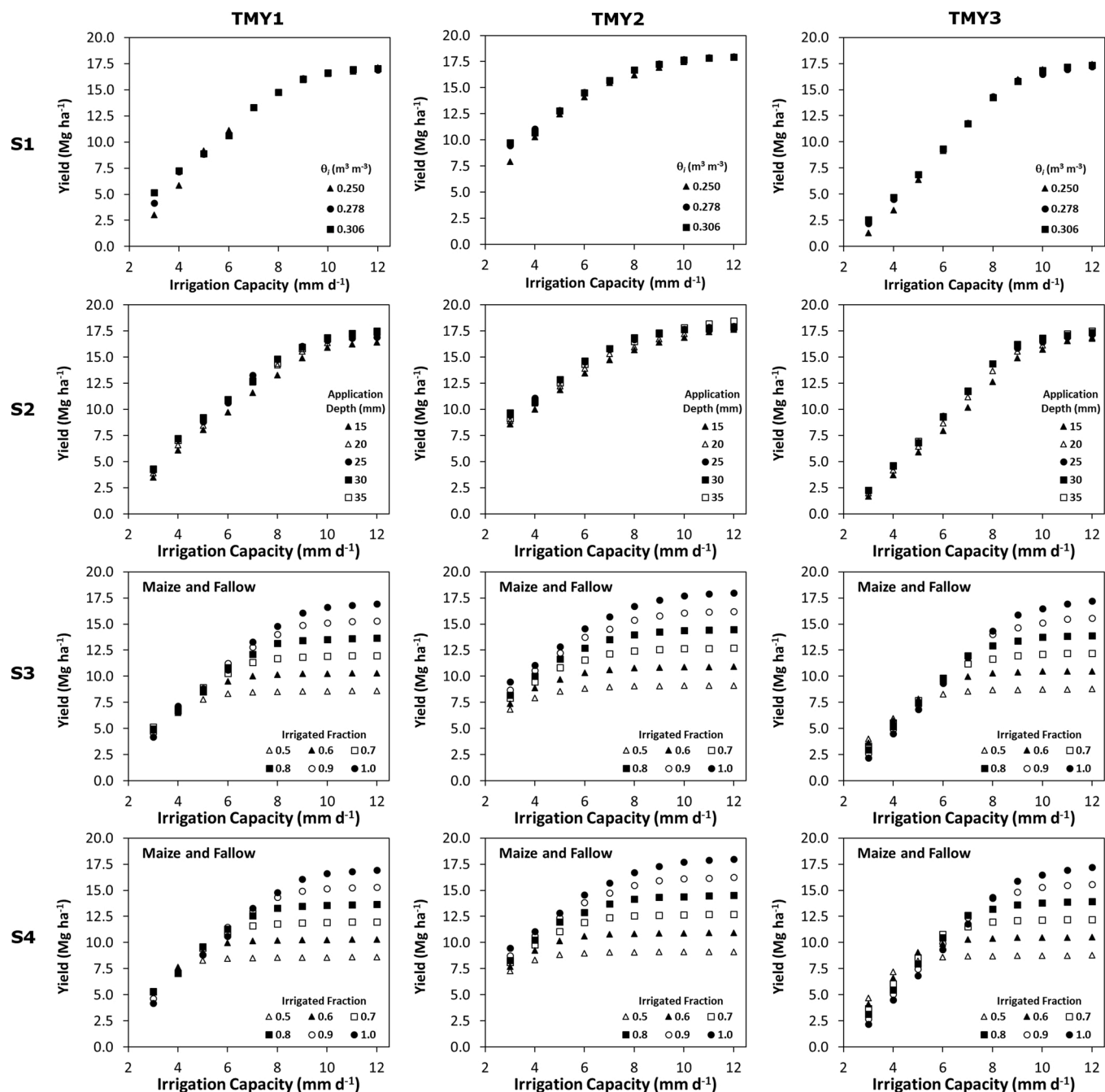


Fig. 6. Grain yield (average of 10 sectors) response to irrigation scenario (rows S1, S2, S3, and S4) and typical meteorological year (columns TMY1, TMY2, and TMY3). Yield is grain yield averaged over the entire area of the pivot even though maize is grown on only the irrigated fraction in S3 and S4. Decline in irrigation capacity during the growing season was set to 15% for all simulations.

typical for the THP, all subsequent results presented assume a 15% decline as detailed in the methods section.

The gross irrigation (Fig. 3) and precipitation received by the crop in combination with the TMY and other factors analyzed in this study (Table 2) determined the overall simulated grain yield of maize per unit of area of the center pivot (Fig. 6). As expected yield declined with reduced irrigation capacity because of the increase in the revolution time of the pivot thereby causing water deficits between irrigation events during some or all of the growth stages. These yield declines are somewhat modified by variable ET demands and rainfall throughout the growing season in combination with the timing of irrigation applications to each sector. Climatic conditions represented by the TMY's affected the range of yields exhibited by differing flow capacities. Thus, under

strategy S1 with an initial water profile water content of  $0.278 \text{ m}^3 \text{ m}^{-3}$  and for growing seasons with normal to above average precipitation (TMY2) the yield ranged from 9.5 to  $18.0 \text{ Mg ha}^{-1}$  depending on the irrigation capacity (Fig. 6). The interval increased from 2.2 to  $17.2 \text{ Mg ha}^{-1}$  under drought conditions (TMY3) decreasing potential yield by 4.3% at the greatest irrigation capacity (Fig. 6). In contrast, when using the whole climatic data base for developing the TMY (TMY1), the minimum yield associated with the lowest capacity was intermediate ( $4.2 \text{ Mg ha}^{-1}$ ) while maximum simulated yield was slightly lower than for TMY3 ( $16.9 \text{ Mg ha}^{-1}$ ) (Fig. 6). Similar effects can be observed in the other strategies. Preseason irrigation of 75 mm, reflected in an increase in profile water content from 0.278 to  $0.306 \text{ m}^3 \text{ m}^{-3}$ , had little to no influence on grain yield at irrigation capacities greater than or equal to

5 mm d<sup>-1</sup> (Fig. 6, S1). Irrigation capacities greater than 5 mm d<sup>-1</sup> were sufficient to overcome soil water deficits at the beginning of the growing season when crop water requirements were low.

Simulated grain yield increased an average of 10% (1.0 Mg ha<sup>-1</sup>) as irrigation application depth increased from 15 to 35 mm under TMY1 (Fig. 6) principally because this facilitated greater seasonal gross and net irrigation. For example, compared with a 15 mm application depth, a 35 mm application depth resulted in an additional 37- and 33- mm average gross and net irrigation, respectively, during the growing season. Yield differences among application depths of 35, 30, and 25 mm were negligible, averaging less than 0.1 Mg ha<sup>-1</sup> under TMY1. Similar results were obtained for TMY2 and TMY3 for grain yield differences between 15 and 35 mm application depths, averaging 0.8 and 1.1 Mg ha<sup>-1</sup>, respectively. Likewise, yield differences among application depths of 35, 30, and 25 mm were negligible for TMY2 and TMY3 (<0.15 Mg ha<sup>-1</sup>). These simulated results assume equivalent irrigation application efficiencies for application depths 25–35 mm. For fine textured soils, slow infiltration rates and poor distribution uniformity (Nascimento et al., 2019) likely compromise these small yield advantages attributed to greater application depths.

Irrigating a fraction of the center pivot area to increase crop water availability in selected sectors (S3) increased average yield of the entire pivot area at the lowest irrigation capacity (3 mm d<sup>-1</sup>) for a year with average precipitation (Fig. 6; S3, TMY1). This slight yield advantage ( $\bar{x}$  = 0.6 Mg ha<sup>-1</sup>) at 3 mm d<sup>-1</sup> occurred for all fractions (0.5–0.9) compared to when the entire pivot was irrigated and peaked at 1.0 Mg ha<sup>-1</sup> at an irrigated fraction of 0.7. At irrigation capacities from 4 to 6 mm d<sup>-1</sup> and irrigated fractions of 0.7–0.9 there were only slight yield differences (0.4–0.6 Mg ha<sup>-1</sup>) compared to when the irrigation volume was spread out over the entire pivot area (Fig. 6; S3, TMY1). Under normal to above average precipitation (TMY2), average yield of the pivot area increased with increasing irrigated fraction for all capacities (Fig. 6; S3, TMY2). Nevertheless, under a seasonal drought (TMY3) and low irrigation capacities ( $\leq 6$  mm day<sup>-1</sup>; 127 m<sup>3</sup> h<sup>-1</sup>), irrigating the entire pivot area resulted in yield reductions (0.2–1.8 Mg ha<sup>-1</sup>) compared to irrigating a fraction (0.6–0.9) (Fig. 6; S3, TMY3). At greater irrigation capacities ( $\geq 7$  mm day<sup>-1</sup>), greater yields could largely be attained by irrigating the total pivot area (Fig. 6; S3, TMY3).

Decreasing the irrigated area by reducing the radius, shutting off nozzles within the final three spans (S4), had a similar effect on yield response across a range of irrigation capacities (Fig. 6; S4) as did irrigating a fraction of the sectors (S3) at all TMY's. Yields associated with

turning nozzles off (S4) were greater compared with yields obtained by irrigating the same fraction by omitting sectors (S3) at low irrigation capacities ( $\leq 6$  mm day<sup>-1</sup>) (Fig. 7). This is primarily due to the irrigation delay associated with moving the pivot through the unirrigated sectors. Although not simulated, improved yields for S4 may also result due to better distribution from maintaining nozzle pressure in response to declines in well yields later in the season (Martin et al., 2019).

#### 3.4. Irrigation water productivity response to irrigation strategies

Irrigation water productivity (IWP) in terms of maize yield increased with flow capacity under all scenarios and all TMY's (Fig. 8). Climatic conditions significantly affected to the range of IWP, which was wider for drought years (TMY3: 0.6–2.5 kg m<sup>-3</sup>) compared with years with normal (TMY1: 1.1–2.7 kg m<sup>-3</sup>) to above average precipitation (TMY2: 2.7–3.3 kg m<sup>-3</sup>). Under scenarios S3 and S4 and under a given TMY, the lowest IWP was obtained with the lowest irrigation capacity when irrigating the entire pivot area. Likewise, the greatest IWP was obtained with the greatest capacity when irrigating half the pivot area.

#### 3.5. Net Revenue under irrigation scenarios

Under long-term average climatic conditions (TMY1), irrigating the entire pivot area resulted in negative net returns at irrigation capacities  $\leq 5$  mm d<sup>-1</sup> (Fig. 9; TMY1, S1-S2). As expected, net returns are less under TMY3, with positive net returns obtained only for irrigation capacities  $\geq 6$  mm d<sup>-1</sup> (Fig. 9; TMY3; S1-S2). However, under TMY2 conditions, all the strategies generated positive net returns regardless of the irrigation capacity (Fig. 9; TMY2; S1-S2).

Irrigating a fraction of the pivot area resulted in greater net returns at capacities  $\leq 8$  mm d<sup>-1</sup> for TMY1 and TMY3 under strategy S4 (Fig. 9). Response of net returns to irrigated fraction under strategy S3 (not shown) were similar to S4 but with slightly lower returns at the lowest irrigation capacity with diminishing differences as irrigation capacity increased. These differences are largely a result of slightly greater maize yields under strategy S4 (Fig. 7). For TMY2 under strategy S4, greater net returns were also attained by irrigating a fraction of the pivot area at irrigation capacities  $\leq 8$  mm d<sup>-1</sup> but only when the unirrigated fraction was planted to dryland cotton. Planting the unirrigated area to cotton resulted in greater net returns under TMY1 and TMY2. In years with a drought during the growing season (TMY3), lint yields were insufficient to offset variable costs associated with cotton production.

At or below the threshold irrigation capacity of 8 mm d<sup>-1</sup> under TMY1, there existed an optimal fraction that maximized net returns which declined with decreasing irrigation capacity (Fig. 10). For example, at an irrigation capacity of 7 mm d<sup>-1</sup>, an irrigation fraction of 0.75 optimized net returns under strategy S4 when the unirrigated fraction was managed as fallow. Corresponding fractions that optimized net returns for S4 with dryland cotton (Fig. 10b) and S3 with fallow (Figs. 10c and 10d) were 0.7 and 0.74, respectively. Achievement of greater net returns by concentrating the water is a consequence of lower yields and lower irrigation water productivities (Fig. 8) combined with the high costs of seed and fertilizer (\$535 to \$721 ha<sup>-1</sup>) and greater variable costs for irrigated (\$992) versus fallow areas (\$88) that are incurred when the entire area is irrigated. The fraction at which the net returns were optimized depended primarily on the growing season precipitation associated with each TMY and was relatively insensitive to commodity prices and input costs. For example, increasing the maize price by 50% and fertilizer costs by 100% for strategy S4 with fallow at an irrigation capacity of 7 mm d<sup>-1</sup> caused the fraction of the maximum of net returns to shift from 0.74 to 0.84 and 0.67, respectively.

Production risks associated with the irrigated fraction can be visualized by simulating net returns for the 1993–2018 climatic data utilized to develop TMY1 (Fig. 10d). The 50% quantile quadratic regression line for this data closely approximates the TMY1 trend. Quantile levels of 30% and 70% as well as the simulated net returns for the 1993–2018

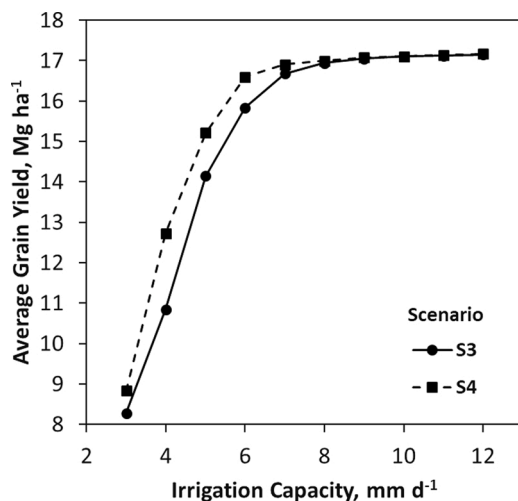
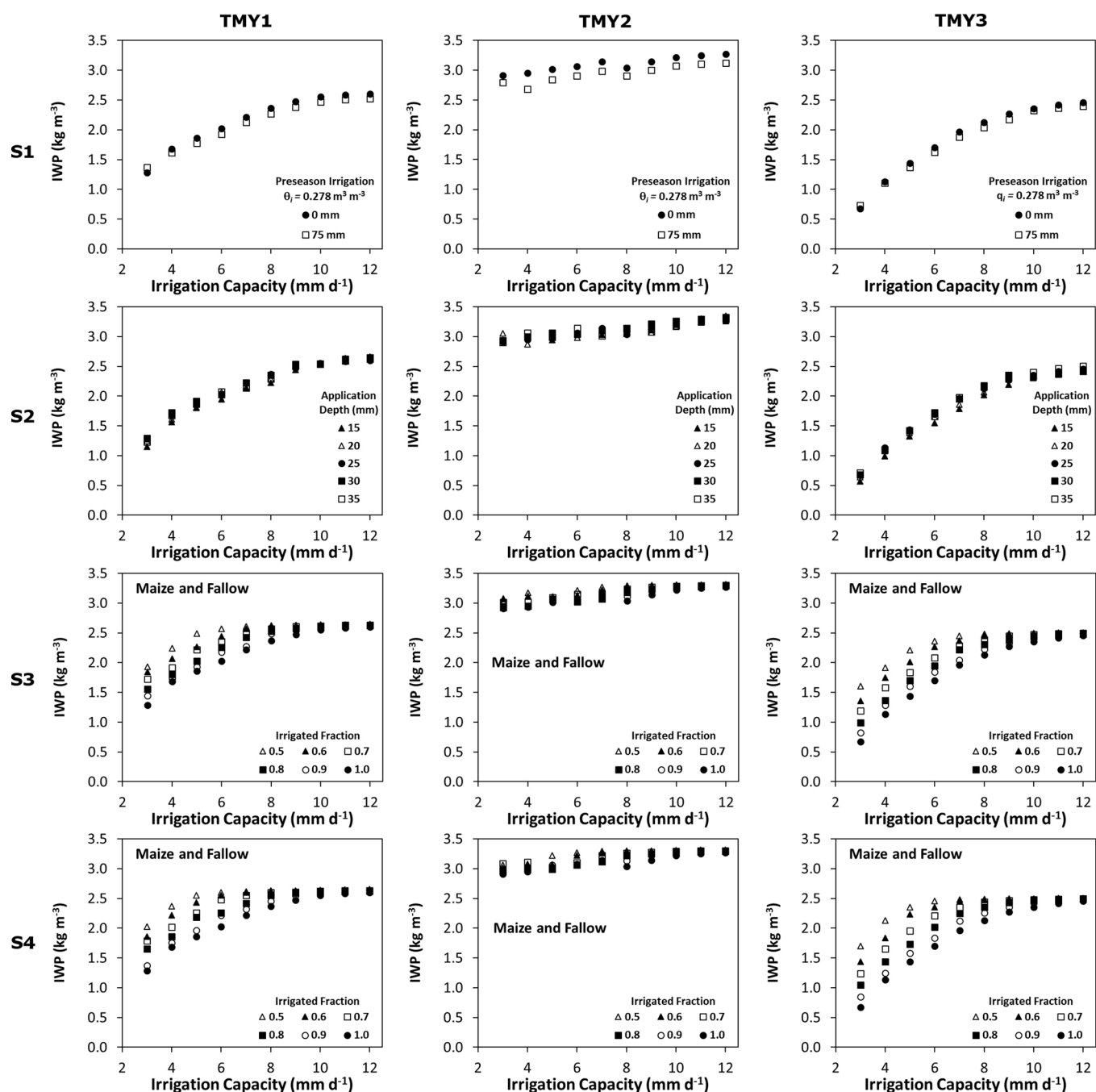


Fig. 7. Simulated yields associated with turning nozzles off in the outer spans (Scenario 4) compared with omitting pivot sectors (Scenario 3) for an irrigated fraction of 0.6. Data were generated assuming a 15% seasonal reduction in irrigation capacity.



**Fig. 8.** Irrigation water productivity (IWP) response to irrigation scenario (rows S1, S2, S3, and S4) and typical meteorological year (columns TMY1, TMY2, and TMY3). Water productivities are based on total maize yield of the entire pivot area divided by the total volume of irrigation water applied irrespective of the irrigated fraction in S3 and S4. Decline in irrigation capacity during the growing season was set to 15% for all simulations.

data unambiguously demonstrate that production risk increases with increasing irrigated fraction.

Maximum irrigation water productivity in terms of net return (IWP, \$ ha<sup>-1</sup>) was attained under TMY1 and TMY2 across all irrigation capacities for strategies where half of the pivot area was irrigated for maize production with the other half planted to dryland cotton (Fig. 11). For TMY3, IWP was greater when the unirrigated area was left in fallow. In this case, irrigating only a fraction of the pivot area resulted in the greatest IWP's for all but the greatest irrigation capacity (12 mm d<sup>-1</sup>).

Applying more seasonal irrigation water did not always generate greater economic benefits. For example, at an irrigation capacity of

7 mm d<sup>-1</sup>, irrigation of 70% of the pivot area with the remaining area in fallow resulted in the application of 455 mm 50.9 ha<sup>-1</sup> seasonal irrigation and generated a net return of \$644 ha<sup>-1</sup> (TMY1 S4). In contrast, irrigation of the entire pivot area with an irrigation capacity of 7 mm d<sup>-1</sup> resulted in the application of 600 mm 50.9 ha<sup>-1</sup> seasonal irrigation and generated a net return of \$458 ha<sup>-1</sup>. Greater net revenues with less water volume resulted in considerably greater irrigation water productivities (\$ m<sup>-3</sup>), especially when the unirrigated area was planted to cotton in years with average (TMY1) and average to above average (TMY2) precipitation (Fig. 11).

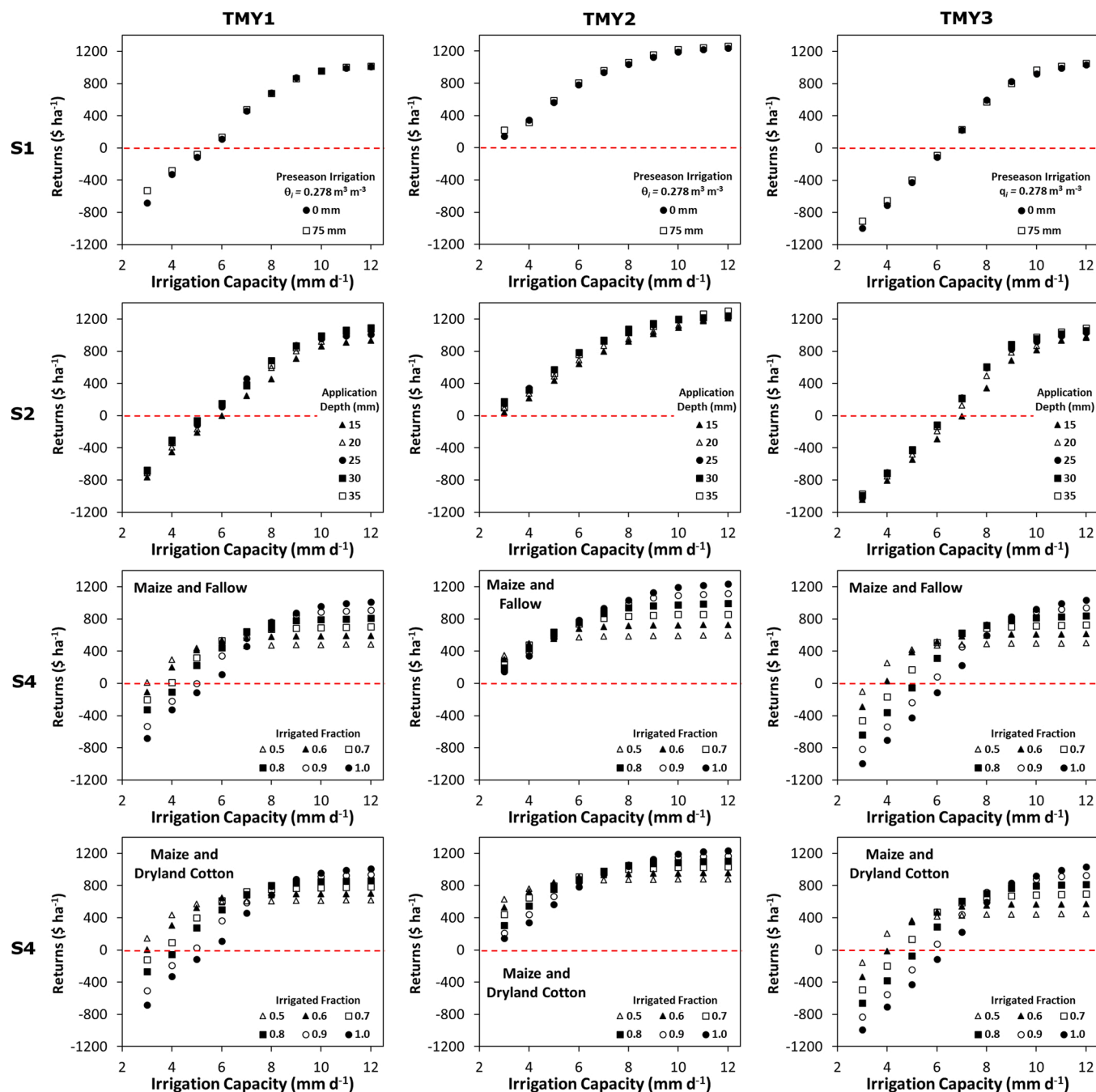


Fig. 9. Net returns in response to irrigation scenario (rows S1, S2, S4 (maize and fallow), and S4 (maize and dryland cotton)) and typical meteorological year (columns TMY1, TMY2, and TMY3). Net returns are based on revenue and variable costs associated with the entire pivot area. Decline in irrigation capacity during the growing season was set to 15% for all simulations.

#### 4. Discussion

Delineating the minimum irrigation capacity for irrigated maize depends on the weather conditions during the growing season, yield potential, and economic considerations (Lamm et al., 2007). Results obtained from our analysis (S1 and S2) suggest that with a yield expectation of 13 Mg ha<sup>-1</sup> (~200 bu ac<sup>-1</sup>) an irrigation capacity of 7 mm d<sup>-1</sup> would be required for growing season with an average amount of precipitation (TMY1). With lower irrigation capacities, simulated yield declines rapidly along with irrigation water productivities. Likewise, a return on investment of greater than 7% in an average growing season requires an irrigation capacity  $\geq 7$  mm d<sup>-1</sup>. This threshold irrigation

capacity is similar to that suggested by Lamm et al. (2007) for northwest Kansas maize production. They simulated yield and net return for irrigated maize and recommended gross irrigation capacities of at least 6.7 mm d<sup>-1</sup> (50% exceedance level) to achieve positive net returns.

Preseason irrigation of 75 mm (that increased profile water content at planting by ~37 mm) resulted in a modest yield increase of 1.0 Mg ha<sup>-1</sup> at a capacity of 3 mm d<sup>-1</sup> but had little to no influence on grain yield at irrigation capacities greater than or equal to 5 mm d<sup>-1</sup>. Irrigation capacities greater than 5 mm d<sup>-1</sup> were sufficient to overcome soil water deficits at the beginning of the growing season when crop water requirements were low and application efficiencies greater. These results are similar to those of the study by Schlegel et al. (2012) in west central

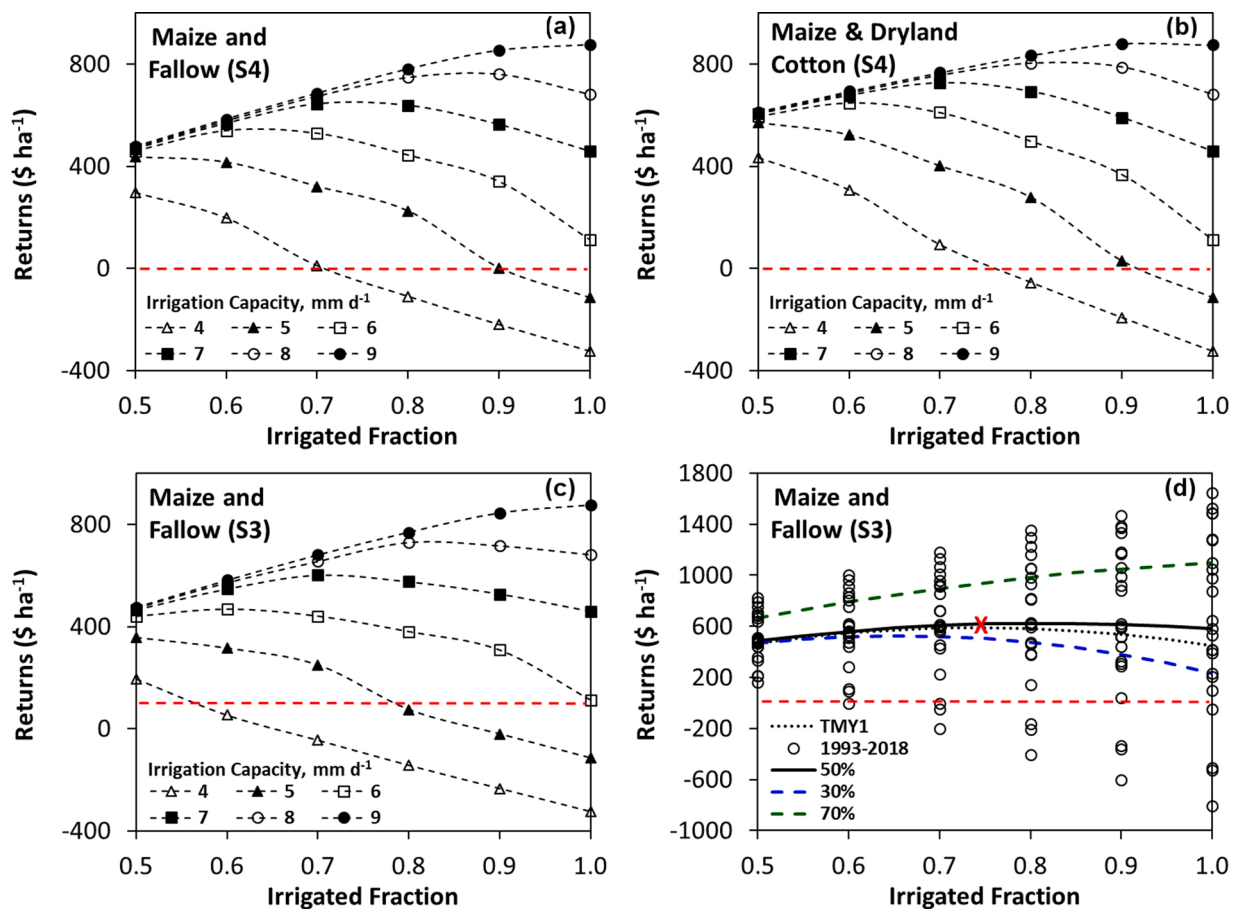


**Fig. 10.** Net returns for a range of irrigation capacities in response to irrigated fraction for typical meteorological year TMY1 and (a) strategy S4 with unirrigated area managed as fallow; (b) strategy S4 with unirrigated area planted to dryland cotton; and (c) strategy S3 with unirrigated area managed as fallow. In (d) the TMY1 trend line for maize and fallow under strategy S3 is shown for an irrigation capacity of 7 mm d<sup>-1</sup> and the corresponding simulated net returns at this capacity for the 1993–2018 climatic data. Also shown are the 50%, 30%, and 70% quantile levels for this data set. The “X” shows the local maximum of the TMY1 trend line. Net returns are based on revenue and variable costs associated with the entire pivot area. Decline in irrigation capacity during the growing season was set to 15% for all simulations.

Kansas that showed increased grain yields of 1.3 Mg ha<sup>-1</sup> with preseason irrigation at capacities of 2.5 and 3.8 mm d<sup>-1</sup>. They concluded that preseason irrigation was unnecessary with irrigation capacities of 5.0 mm d<sup>-1</sup> or greater.

With irrigation capacities  $\leq 8$  mm d<sup>-1</sup> in a year with average growing season precipitation (TMY1), reducing the irrigated area is the most prudent option for optimizing net returns under maize production. Reducing the area of the irrigated circle by turning off nozzles in the outer spans (S4) resulted in greater yields compared with omitting irrigation in sectors of the pivot area (S3). This also has the advantage of maintaining system pressure and reducing problems with application uniformity associated with supplying water to all spans under reduced flows (Martin et al., 2019). Planting dryland cotton in the unirrigated fraction improved net returns under TMY1 and TMY2 but not for a growing season with a drought (TMY3). Because greater applications of seasonal irrigation water did not always generate greater economic benefits, there is the opportunity for producers to both increase net returns and save water under reduced irrigation capacities by irrigating a fraction of the pivot area.

Evaluations of yield and net revenue response to irrigating a fraction of the land area compared to the entire pivot area at fixed flow capacities are limited in the southern U.S. Great Plains. Klocke et al. (2006) introduced a water allocation model for limited irrigation to a range of crops but a detailed analysis of results for irrigated maize was not

presented. Using AquaCrop (Raes et al., 2009) to estimate yields over a range of irrigation capacities in southwestern Kansas, Araya et al. (2017) inferred that maize yields could be optimized for a sandy clay loam by plating 75% of the area of a typical center pivot system compared to 50% and 100% of the area for irrigation capacities of 3.3 mm d<sup>-1</sup> during a “dry” growing season (182 mm precipitation). For a silt loam soil, yield optimization at 3.3 mm d<sup>-1</sup> was obtained by planting the entire pivot area. Assuming no seasonal decline in irrigation capacity as did Araya et al. (2017), our results indicate that yield advantages of planting 50% of the pivot extended to 4 mm d<sup>-1</sup> for a growing season with a drought (TMY3; 100 mm precipitation) in an environment with greater ET demand. For TMY2 (growing precipitation = 158) yield was maximized at 0.7–0.8 of the area irrigated at a capacity of 3 mm d<sup>-1</sup>. In this case, our yield optimizations that occur at smaller fractions of the pivot area at low capacities compared to that of Araya et al. (2017) for the silt loam soil reflect the greater seasonal  $ET_0$  in the THP compared to southwestern Kansas. Simulated yield declines in the THP are steeper thereby penalizing the spreading of water. We also note that dryland maize production is common in western Kansas yet considered unfeasible in the THP.

Foster et al. (2015) also modeled effects of maize yield and profitability using AquaCrop for the Texas High Plains (Amarillo) to predict the optimum fraction of an irrigated area over a range of irrigation capacities. For irrigation capacities of 3.8, 5.7, and 7.6 mm d<sup>-1</sup>, net returns

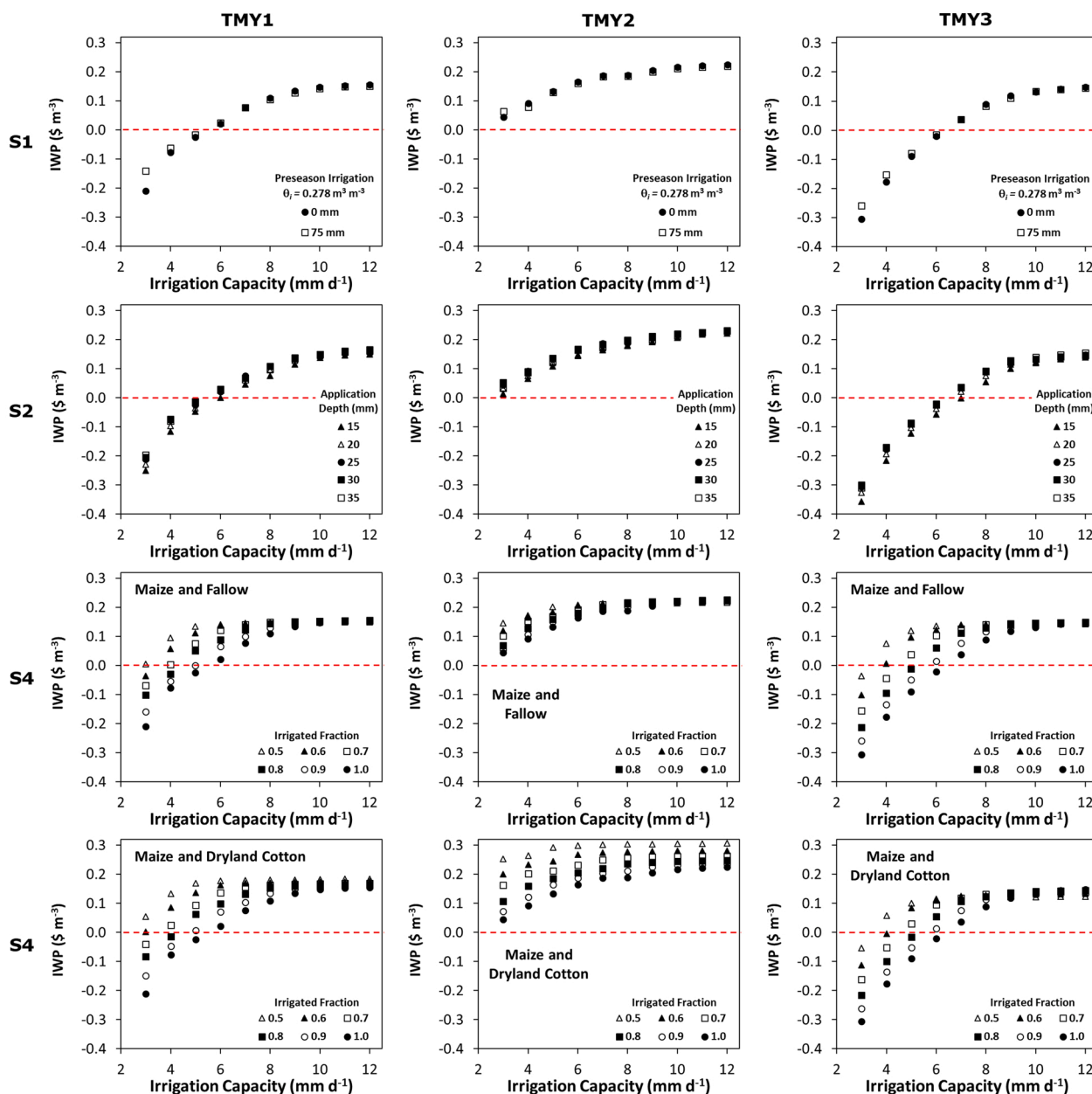


Fig. 11. Irrigation water productivity (IWP) response to irrigation scenario (rows S1, S2, S4 (maize and fallow), and S4 maize and dryland cotton) and typical meteorological year (columns TMY1, TMY2, and TMY3). Water productivities are based on net revenue associated with the entire pivot area divided by the total volume of irrigation water applied irrespective of the irrigated fraction in S3 and S4. Decline in irrigation capacity during the growing season was set to 15% for all simulations.

were optimized at irrigated fractions of 0.32, 0.51, and 0.72. In contrast, our results indicated net returns are optimized at similar irrigation capacities with greater irrigated fractions (e.g. at 4 and 6 mm d<sup>-1</sup> net returns were optimized with irrigated fractions of 0.5 and 0.6, respectively). Our results show that the transitional point where irrigating the entire pivot area became most profitable occurred at 9 mm d<sup>-1</sup> whereas this threshold was determined to occur at 11.4 mm d<sup>-1</sup> by Foster et al. (2015). Noting the relative insensitivity of the optimum fraction to maize prices and costs discussed earlier, this apparent inconsistency with regards to our study is likely explained by the fact that Foster et al. (2015) did not consider the timing of irrigation applications to the entire

pivot area. For example, 700 mm of seasonal irrigation to maize was achieved with an irrigation capacity of 5 mm d<sup>-1</sup> (Foster et al. (2015) whereas considering the logistics of applying irrigation at this rate, our seasonal irrigation was limited to 525 mm. We also note that the crop model used by Foster et al. (2015) was not calibrated for the region. Clearly, the inability of previous modelling assessments at low irrigation capacities to explicitly account for constraints associated with timing of irrigations and moving the pivot through unirrigated sectors under restricted irrigation capacities may result in unreliable predictions of yield and profitability.

The foregoing analyses assumes that well pumping capacities are

limited as a result of aquifer characteristics. However, in many areas of the High Plains Aquifer, annual well production limits are established by groundwater districts or producer organizations. For instance, the Texas High Plains Water District (High Plains Water District, 2020b) limits the total amount of production to 457 mm (18 in.) per contiguous land area per year. This level of production equates to an irrigation capacity of approximately 7 – 8 mm d<sup>-1</sup> in a normal (TMY1) year for a pivot contained with a quarter section (65 ha). Newly permitted wells in the THP for which well production observations are available (High Plains Water District, 2020a) indicate that 83% had pumping flow rates less than 60 m<sup>3</sup> h<sup>-1</sup> which is equivalent to an irrigation capacity of approximately 2.8 mm d<sup>-1</sup> if water was spread out over 50.9 ha. Obviously, within this groundwater district, irrigation capacities greater than 7 mm d<sup>-1</sup> are not common because of limited well production relative to the land area available for irrigated cultivation. In such cases, well production restrictions established by the groundwater district would not influence how water allocation decisions are made to optimize net return using our analysis. In cases where the producer has irrigation capacities that exceed limits on pumping set by established rules, optimization of maize yield and net returns will need to consider the approach presented by Domínguez et al. (2012a, 2017) or Bell et al. (2018) in which the volume of water pumped is limited yet proportionately greater volumes of irrigation are applied during the early reproductive phases that are most sensitive to water stress.

Because producers do not have the necessary knowledge of weather conditions and accurate forecasts during the growing season in advance of planting, decisions will unavoidably involve risks associated with the fraction of the area that is irrigated. Irrigating a smaller fraction can result in significant opportunity costs if the year is wetter than average. Planting a larger area with the expectation for a wetter season can result in significant economic losses when precipitation is below normal. Our simulated results suggest that under limiting capacities, opportunity costs can be minimized and net returns optimized for an average year (TMY1) by planting dryland cotton in unirrigated areas. In years with seasonal droughts, forecasting well before planting time (March) is necessary for producers to respond with appropriate irrigation practices to mitigate potential losses. The proposed method using TMY3 to assess irrigation strategies in conjunction with drought forecasts being implemented by the Texas Water Development Board (Fernando et al., 2019) would provide actionable information for producers and also crop insurance provider's to adjust the planted acreage, reduce crop failures, and stabilize profit. The combination of optimizing spatial allocation of water to crops (López-Mata et al., 2016) with weather forecasting (Politi et al., 2018) is being promoted in other areas of the world, as is the case of the SUPROMED project (www.supromed.eu) within the Mediterranean basin.

## 5. Conclusions

The MOPECO crop model adapted to simulate maize water use and yield under center pivot irrigation in conjunction with the Typical Meteorological Year approach was useful in delineating the optimal irrigation strategies that maximized net return under limited irrigation capacities. Inclusion of algorithms to schedule irrigation that considered actual constraints associated with moving the pivot through a field resulted in lower but more realistic yields compared with simulations without such restrictions.

Although maize yields for the entire pivot area in an average rainfall year were predicted to be greater than or marginally less (1 Mg ha<sup>-1</sup>) when the entire pivot area was cropped compared to a fraction, reducing the irrigated area was the most prudent option for optimizing net returns under maize production when irrigation capacity was limiting ( $\leq 8$  mm d<sup>-1</sup>). Greater net returns achieved with concentrating the water was a consequence of greater irrigation water productivities combined with the lower seed and fertilizer costs resulting from reduced maize-cropped land area. Greater applications of seasonal irrigation water did not

always generate greater net returns and therefore there is an opportunity to both increase net returns and save water by irrigating a fraction of the pivot area.

With the crop production revenue and variable costs used in this study, at an irrigation capacity of 3 mm d<sup>-1</sup>, net returns were on average negative even when only half the pivot area was planted to maize. At irrigation capacities from 4 to 5 mm d<sup>-1</sup>, net returns were optimized when approximately half the pivot area was irrigated. For an irrigation capacity of 7 mm d<sup>-1</sup>, typical of the THP, net returns were optimized when approximately 75% of the pivot area was irrigated. Planting cotton in the unirrigated portion increased net returns except in years with a seasonal drought (TMY3). The optimal irrigated fraction that maximized net returns depended principally on growing season precipitation and was relatively insensitive to maize prices and input costs. Because of the potentially large economic losses under maize production that occur in years with seasonal drought, accurate climatic forecasting would be indispensable in conjunction with these simulations to determine optimum irrigation strategies well in advance of planting.

## Declaration of Competing Interest

The authors declare that they have no known competing financial interests or personal relationships that could have appeared to influence the work reported in this paper.

## Acknowledgements

The authors gratefully acknowledge the efforts of Karen Copeland for maintaining and providing long-term weather data used in this study. R. C. Schwartz and A. Domínguez acknowledge the receipt of a fellowship from the OECD Co-operative Research Programme: Biological Resource Management for Sustainable Agricultural Systems in 2017 and 2018, respectively. This research was supported in part by the Ogallala Aquifer Program, a consortium between USDA Agricultural Research Service, Kansas State University, Texas A&M AgriLife Research, Texas A&M AgriLife Extension Service, Texas Tech University, and West Texas A&M University. The methodologies utilized in this paper were developed within the framework of several projects (SUPROMED "GA-1813" funded by PRIMA, and AGL2017-82927-C3-3-R funded by the Spanish Research Agency co-financed with European Union ERDF Funds).

## References

- Agnew, C.T., 2000. Using the SPI to Identify Drought. International Drought Information Center and the National Drought Mitigation Center, School of Natural Resources, University of Nebraska, Lincoln NE. (<https://digitalcommons.unl.edu/droughtmetnews/1/>).
- Araya, A., Kisekka, I., Vara Prasad, P.V., Gowda, P., 2017. Evaluating optimum limited irrigation management strategies for corn production in the Ogallala Aquifer region. *J. Irrig. Drain. Eng.* 143, 04017041 [https://doi.org/10.1061/\(asce\)ir.1943-4774.0001228](https://doi.org/10.1061/(asce)ir.1943-4774.0001228).
- ASCE, 2005. In: Allen, R.G., Walter, I.A., Elliot, R.L., Howell, T.A. (Eds.), *The ASCE Standardized Reference Evapotranspiration Equation*. ASCE Press, Reston, VA.
- Bell, J.M., Schwartz, R.C., McInnes, K.J., Howell, T.A., Morgan, C.L., 2018. Deficit irrigation effects on yield and yield components of grain sorghum. *Agric. Water Manag.* 203, 289–296. <https://doi.org/10.1016/j.agwat.2018.03.002>.
- Baumhardt, R.L., Staggenborg, S.A., Gowda, P.H., Colaizzi, P.D., Howell, T.A., 2009. Modeling irrigation management strategies to maximize cotton lint yield and water use efficiency. *Agron. J.* 101, 460–468. <https://doi.org/10.2134/agronj2008.0041xs>.
- Baumhardt, R.L., Tolk, J.A., Howell, T.A., Rosenthal, W.D., 2007. Sorghum management practices suited to varying irrigation strategies: a simulation analysis. *Agron. J.* 99, 665–672. <https://doi.org/10.2134/agronj2006.0092>.
- Benavidez, J., Jones, D., Almas, L., Guerrero, B., Crouch, M., 2019. Texas Crops and Livestock Budgets, Texas High Plains, Projected for 2020. December, 2019. B-1241, Texas A&M AgriLife Extension Service, College Station, Texas. <https://agecoext.tamu.edu/resources/crop-livestock-budgets/budgets-by-extension-district/district-1-panhandle/> (Accessed November 2021).
- Benavidez, J., Jones, D., Guerrero, B., García, L., 2020. Texas Crop and Livestock Budgets, Texas High Plains, Projected for 2021. December, 2020. Texas A&M AgriLife Extension Service, College Station, Texas. <https://agecoext.tamu.edu/resources/crop-livestock-budgets/budgets-by-extension-district/district-1-panhandle/> (Accessed November 2021).

- Colaizzi, P., Gowda, P., Marek, T., Porter, D., 2009. Irrigation in the Texas High Plains: a brief history and potential reductions in demand. *Irrig. Drain.* 58, 257–274. <https://doi.org/10.1002/ird.418>.
- Crouch, M., Guerrero, B., Amosson, S., Marek, T., Almas, L., 2020. Analyzing potential water conservation strategies in the Texas Panhandle. *Irrig. Sci.* 38, 559–567. <https://doi.org/10.1007/s00271-020-00691-2>.
- Domínguez, A., de Juan, J.A., Tarjuelo, J.M., Martínez, R.S., Martínez-Romero, A., 2012a. Determination of optimal regulated deficit irrigation strategies for maize in a semi-arid environment. *Agr. Water Manag.* 110, 67–77. <https://doi.org/10.1016/j.agwat.2012.04.002>.
- Domínguez, A., Martínez, R.S., de Juan, J.A., Martínez-Romero, A., Tarjuelo, J.M., 2012b. Simulation of maize crop behavior under deficit irrigation using Mopeco model in a semi-arid environment. *Agr. Water Manag.* 107, 42–53. <https://doi.org/10.1016/j.agwat.2012.01.006>.
- Domínguez, A., Martínez-Navarro, A., López-Mata, E., Tarjuelo, J.M., Martínez-Romero, A., 2017. Real farm management depending on the available volume of irrigation water (part I): financial analysis. *Agric. Water Manag.* 192, 71–84. <https://doi.org/10.1016/j.agwat.2017.06.022>.
- Domínguez, A., Martínez-Romero, A., Leite, K.N., Tarjuelo, J.M., de Juan, J.A., López-Urrea, R., 2013. Combination of typical meteorological year with regulated deficit irrigation to improve the profitability of garlic in central Spain. *Agric. Water Manag.* 130, 154–167. <https://doi.org/10.1016/j.agwat.2013.08.024>.
- Doorenbos, J., Kassam, A.H., 1979. Yield Response to Water. *Irrig. and Drain. Paper No. 33*, Food and Agric. Org. United Nations, Rome, Italy, pp. 192.
- FAO, 1998. Crop Evapotranspiration: Guidelines for computing crop water requirements. In: Allen, R.G., Pereira, L.S., Raes, D., Smith, M. (Eds.), *Irrigation and Drainage. Food and Agriculture Organization of the United Nations, Rome*, p. 300. Paper 56.
- Fernando, D.N., Chakraborty, S., Fu, R., Mace, R.E., 2019. A process-based statistical seasonal prediction of May–July rainfall anomalies over Texas and the Southern Great Plains of the United States. *Clim. Serv.* 16, 100133 <https://doi.org/10.1016/j.cliser.2019.100133>.
- Foster, T., Brozović, N., Butler, A.P., 2015. Why well yield matters for managing agricultural drought risk. *Weather Clim. Extrem.* 10, 11–19. <https://doi.org/10.1016/j.wace.2015.07.003>.
- Hall, L.J., Prairie, R.R., Anderson, H.E., Boes, E.C., 1978. Generation of Typical Meteorological Years for 26 SOL-MET Stations. Sandia National Laboratories, Albuquerque, NM.
- High Plains Water District, 2020a. Annual Report. High Plains Underground Water District No. 1, Lubbock, Texas 79411. (<http://www.hpwd.org/reports>) (Accessed November 2021).
- High Plains Water District, 2020b. Rules of the High Plains Water District. Adopted 24 Nov., 2020. High Plains Underground Water District No. 1, Lubbock, Texas 79411. (<http://www.hpwd.org/reports>) (Accessed November 2021).
- Howell, T.A., 2003. Irrigation efficiency. In: Stewart, B.A., Howell, T.A. (Eds.), *Encyclopedia of Water Science*. Marcel Dekker, New York, pp. 467–472.
- Howell, T.A., Evett, S.R., Tolk, J.A., Schneider, A.D., Steiner, J.L., 1996. Evapotranspiration of corn – southern high plains. In: Camp, C.R., Sadler, E.J., Yoder, R.E. (Eds.), *Evapotranspiration and Irrigation Scheduling*. American Society of Agricultural Engineering, St. Joseph, MI, San Antonio, TX, pp. 158–166.
- Howell, T.A., Steiner, J.L., Schneider, A.D., Evett, S.R., 1995a. Evapotranspiration of irrigated winter wheat—southern high plains. *Trans. ASAE* 38, 745–775. <https://doi.org/10.13031/2013.27888>.
- Howell, T.A., Yazar, A., Schneider, A., Dusek, D., Copeland, K., 1995b. Yield and water use efficiency of corn in response to LEPA irrigation. *Trans. ASAE* 38, 1737–1747. <https://doi.org/10.13031/2013.28001>.
- Jones, D., Almas, L., Guerrero, B., Amosson, S., Crouch, M., Wagner, J., 2018. Texas Crops and Livestock Budgets, Texas High Plains, Projected for 2019. December, 2018. B-1241, Texas A&M AgriLife Extension Service, College Station, Texas. 87 pp. <https://agecoext.tamu.edu/resources/crop-livestock-budgets/budgets-by-extension-district/district-1-panhandle/> (Accessed November 2021).
- Klocke, N.L., Stone, L.R., Clark, G.A., Dumler, T.J., Briggeman, S., 2006. Water allocation model for limited irrigation. *Appl. Eng. Agric.* 22, 381–389. <https://doi.org/10.13031/2013.20458>.
- Lamm, F.R., Stone, L.R., O'Brien, D.M., 2007. Crop production and economics in northwest Kansas as related to irrigation capacity. *Appl. Eng. Agric.* 23, 737–745. <https://doi.org/10.13031/2013.24057>.
- López-Mata, E., Orengo-Valverde, J.J., Tarjuelo, J.M., Martínez-Romero, A., Domínguez, A., 2016. Development of a direct-solution algorithm for determining the optimal crop planning of farms using deficit irrigation. *Agric. Water Manag.* 171, 173–187. <https://doi.org/10.1016/j.agwat.2016.03.015>.
- Mahan, J.R., Lascano, R.J., 2016. Irrigation analysis based on long-term weather data. *Agriculture* 6, 42. <https://doi.org/10.3390/agriculture6030042>.
- Martin, D., Heeren, D., Melvin, S., Ingram, T., 2019. Effect of limited water supplies on center pivot performance (pp. 71–97). Proceedings 31st Annual Central Plains Irrigation Conference, Kearney, NE, 26–27 Feb. 2019. (<https://www.ksr.k-state.edu/irrigate/oow/p19/Martin19.pdf>) (Accessed November 2021).
- McGuire, V.L., 2009. Water-level changes in the High Plains aquifer, predevelopment to 2007, 2005–06, and 2006–07: U.S. Geological Survey Scientific Investigations Report 2009–5019, 9 p. (<http://pubs.usgs.gov/sir/2009/5019/>) (Accessed November 2021).
- McGuire, V.L., 2017. Water-level and recoverable water in storage changes, High Plains aquifer, predevelopment to 2015 and 2013–15: U.S. Geological Survey Scientific Investigations Report 2017–5040, 14 p. (<https://doi.org/10.3133/sir20175040>).
- McMaster, G.S., Wilhelm, W.W., 1997. Growing degree days: one equation two interpretations. *Agric. For. Meteorol.* 87, 291–300. [https://doi.org/10.1016/S0168-1923\(97\)00027-0](https://doi.org/10.1016/S0168-1923(97)00027-0).
- Nascimento, A.K., Schwartz, R.C., Lima, F.A., López-Mata, E., Domínguez, A., Izquier, A., Tarjuelo, J.M., Martínez-Romero, A., 2019. Effects of irrigation uniformity on yield response and production economics of maize in a semiarid zone. *Agric. Water Manag.* 211, 178–189. <https://doi.org/10.1016/j.agwat.2018.09.051>.
- North Plains Groundwater Conservation District, 2012. 200 – 12 Reduced Irrigation on Corn Demonstration Project. ([http://northplainsgcd.org/wp-content/uploads/200-12-Report-Final-2012\\_smaller.pdf](http://northplainsgcd.org/wp-content/uploads/200-12-Report-Final-2012_smaller.pdf)) (Accessed November 2021).
- North Plains Groundwater Conservation District, 2020. Continuous Well Monitoring Network of the North Plains Groundwater Conservation District. (<http://map.northplainsgcd.org/#>) (Accessed November 2021).
- Ortega, J.F., de Juan, J.A., Tarjuelo, J.M., López-Mata, E., 2004. MOPECO: an economic optimization model for irrigation water management. *Irrig. Sci.* 23, 61–75. <https://doi.org/10.1007/s00271-004-0094-x>.
- Politi, N., Nastos, P.T., Sfetsos, A., Vlachogiannis, D., Dalezios, N.R., 2018. Evaluation of the AWR-WRF model configuration at high resolution over the domain of Greece. *Atmos. Res.* 208, 229–245. <https://doi.org/10.1016/j.atmosres.2017.10.019>.
- Pu, B., Fu, R., Dickinson, R.E., Fernando, D.N., 2016. Why do summer droughts in the Southern Great Plains occur in some La Nina years but not others? *J. Geophys. Res. Atmos.* 121, 1120–1137. <https://doi.org/10.1002/2015JD023508>.
- Raes, D., Steduto, P., Hsiao, T.C., Fereres, E., 2009. AquaCrop—the FAO crop model to simulate yield response to water: II. Main algorithms and software description. *Agron. J.* 101, 438–447. <https://doi.org/10.2134/agronj2008.0140s>.
- Rallison, R.E., 1980. Origin and Evolution of the SCS Runoff Equation. ASCE, New York, pp. 912–924 (Symp. on Watershed Manage).
- Rao, N.H., Sarma, P.B.S., Chander, S., 1988. A simple dated water-production function for use in irrigated agriculture. *Agric. Water Manag.* 13, 25–32. [https://doi.org/10.1016/0378-3774\(88\)90130-8](https://doi.org/10.1016/0378-3774(88)90130-8).
- Scanlon, B.R., Faunt, C.C., Longuevergne, L., Reedy, R.C., Alley, W.M., McGuire, V.L., McMahon, P.B., 2012. Groundwater depletion and sustainability of irrigation in the US High Plains and Central Valley. *Proc. Natl. Acad. Sci.* 109 (24), 9320–9325. <https://doi.org/10.1073/pnas.1200311109>.
- Schlegel, A.J., Stone, L.R., Dumler, T.J., Lamm, F.R., 2012. Managing diminished irrigation capacity with preseason irrigation and plant density for corn production. *Trans. ASABE* 55, 525–531. <https://doi.org/10.13031/2013.41394>.
- Schneider, A.D., Howell, T.A., 1998. LEPA and spray irrigation of corn—southern high plains. *Trans. ASAE* 41, 1391–1396. <https://doi.org/10.13031/2013.17313>.
- Schwartz, R.C., Domínguez, A., Pardo, J.J., Colaizzi, P.D., Baumhardt, R.L., Bell, J.M., 2020a. A crop coefficient –based water use model with non-uniform root distribution. *Agric. Water Manag.* 228, 105892 <https://doi.org/10.1016/j.agwat.2019.105892>.
- Schwartz, R.C., Witt, T.W., Ulloa, M., Colaizzi, P.D., Baumhardt, R.L., 2020b. Water use, yield, and fiber quality response of six upland cotton cultivars to irrigation. Proc. of the 2020 Beltwide Cotton Conferences, Austin, TX, January 8–10, 2020. National Cotton Council of America. (<https://www.cotton.org/beltwide/proceedings/2005-2021/index.htm>) (Accessed November 2021).
- Stewart, J.I., Danielson, R.E., Hanks, R.J., Jackson, E.B., Hagan, R.M., Pruitt, W.O., Franklin, W.T., Riley, J.P., 1977. Optimizing crop production through control of water and salinity levels in the soil. Utah Water Lab, PRWG 151–1. pp. 191. [https://digitalcommons.usu.edu/water\\_rep/67/](https://digitalcommons.usu.edu/water_rep/67/) (Accessed November 2021).
- Stout, J.E., 2018. Seasonal water-level perturbations beneath the high plains of the Llano Estacado. *J. Hydrol. Reg. Stud.* 18, 1–14. <https://doi.org/10.1016/j.ejrh.2018.04.009>.
- Tolk, J.A., Evett, S.R., Schwartz, R.C., 2015. Field-measured, hourly soil water evaporation stages in relation to reference evapotranspiration rate and soil to air temperature ratio. *Vadose Zone J.* <https://doi.org/10.2136/vzj2014.07.0079>.
- Xue, Q., Marek, T.H., Xu, W., Bell, J.M., 2017. Irrigated corn production and management in the Texas High Plains. *J. Contemp. Water Res. Educ.* 162, 31–41. <https://doi.org/10.1111/j.1936-704X.2017.03258.x>.